



Research article

Carbamate insecticide bendiocarb induces complex embryotoxic effects, including morphological, behavioral, transcriptional, and immunological alterations in zebrafish

Bence Ivánovics^{a,1}, Gyöngyi Gazsi^{a,1}, Zoltán K. Varga^b, Ádám Staszny^a, Eszter Váradi^{c,d}, Zsófia Varga^c, András Ács^{a,e}, Márta Tóth^{f,g}, Apolka Domokos^{h,i}, Márta Reining^a, Erna Vásárhelyi^a, Szilárd Póliska^j, Róbert Kovács^a, Ferenc Baska^k, Zoltán Filep^l, Attila Bácsi^f, Julianna Kobolák^a, Béla Urbányi^{a,m}, István Szabó^a, Tamás Müller^a, Zsolt Csenki-Bakos^{a,*}, Zsolt Czimmerer^{c,*}

^a Institute of Aquaculture and Environmental Safety, Hungarian University of Agriculture and Life Sciences, H-2100, Godollo, Hungary

^b Translational Behavioral Neuroscience Research Group, HUN-REN Institute of Experimental Medicine, Budapest, Hungary

^c HUN-REN Biological Research Centre, Institute of Genetics, Szeged, Hungary

^d Doctoral School in Biology, University of Szeged, Szeged, Hungary

^e Ecophysiological and Environmental Toxicological Research Group, HUN-REN Balaton Limnological Research Institute (HUN-REN), 8237, Tihany, Hungary

^f Department of Immunology, Faculty of Medicine, University of Debrecen, Debrecen, Hungary

^g Division of Pediatric Allergy/Immunology, University of South Florida at Johns Hopkins All Children's Hospital, St. Petersburg, FL 33701, USA

^h Department of Biochemistry and Molecular Biology, Faculty of Medicine, University of Debrecen, Debrecen, Hungary

ⁱ Doctoral School of Molecular Cell and Immune Biology, University of Debrecen, Debrecen, Hungary

^j Genomic Medicine and Bioinformatic Core Facility, Department of Biochemistry and Molecular Biology, Faculty of Medicine, University of Debrecen, Debrecen, Hungary

^k Department of Exotic Animal and Wildlife Medicine, University of Veterinary Medicine, Budapest, Hungary

^l Eurofins Analytical Services Hungary Ltd, Budapest, Hungary

^m University of Győr, Faculty of Albert Kázmér, Mosonmagyaróvár, Vár u. 2., 9200

ARTICLE INFO

Edited by Martin Grosell

Keywords:

Carbamate
Developmental toxicity
Behavioral alterations
Immunotoxicity
Zebrafish embryo

ABSTRACT

The emergence and spread of vector-borne diseases necessitate the increased use of insecticides, such as carbamates, raising concerns about their potential toxicological risks to non-target organisms, including humans. Bendiocarb, frequently applied in indoor spraying operations and detected in maternal and fetal circulation, warrants particular attention for its developmental toxicity. This study aimed to assess transcriptional and phenotypic effects of sublethal bendiocarb exposure at concentrations of 0.035, 0.2, 0.4, 0.75, and 1.5 mg/L, using zebrafish embryos, a vertebrate model for developmental toxicity testing. Our analyses revealed acetylcholinesterase inhibition-associated morphological and behavioral abnormalities, including reduced locomotor activity in response to both visual and tactile stimuli, as well as impaired non-associative learning. Transcriptomic analysis indicated activation of muscle, immune, and metabolic pathways, while neurodevelopmental, phototransduction, and cell proliferation processes were suppressed. Consistent with these molecular findings, structural damage was observed in the retina, skeletal muscle, and notochord. Furthermore, bendiocarb exposure disrupted neutrophil granulocyte distribution and impaired inflammatory responses. Altogether, our results provide new insights into the embryotoxic effects of bendiocarb, highlighting its potential to disrupt early vertebrate development. These findings provide mechanistic insight that may support more informed evaluations of potential public health risks associated with developmental exposure to carbamates.

* Corresponding authors.

E-mail addresses: csenki-bakos.zsolt.imre@uni-mate.hu (Z. Csenki-Bakos), czimmerer.zsolt@brc.hu (Z. Czimmerer).

¹ These authors contributed equally to this work.

1. Introduction

Climate change-driven temperature anomalies and habitat alterations are expected to significantly affect the epidemiology of insect-borne diseases (Brugueras et al., 2020; Caminade et al., 2019). In addition, the adaptation of arthropod vectors to changing environmental conditions can co-evolve with their resistance to insecticides (Pu et al., 2020). These changes entail more intensive use of vector control chemicals containing compounds with different mechanisms of action, resulting in an increased risk to humans and non-target animals (van den Berg et al., 2021). The potential health risks associated with pesticides are particularly significant if the exposure occurs during early-life periods, especially during critical stages of embryonic development in vertebrates, including humans (Addissie et al., 2020; Ait-Bali et al., 2016; Amstislavsky et al., 2003; Ding et al., 2024; Garry et al., 2002; Gely-Pernot et al., 2017; Ishido et al., 2017; Manikkam et al., 2014; Suarez-Lopez et al., 2013).

N-methyl carbamates are among the most commonly used insecticides against pests and disease vectors. Their primary target is the arthropod nervous system through the reversible inhibition of acetylcholinesterase (AChE), forming a covalent bond with a serine residue of the enzyme (Lee and Barron, 2016). However, the most commonly used commercially available carbamates exhibit a less specific AChE-inhibitory activity, which can potentially have a neurotoxic effect in vertebrates, posing a threat to embryonic development as well (Jiang et al., 2013; Tsiaoussis et al., 2018). Abnormal neurogenesis (Mishra et al., 2012; Ostrea et al., 2012), impaired myelination (Seth et al., 2019), defective motor function (An et al., 2023a; Kamboj et al., 2006), behavioral alterations (Jablonski et al., 2022) and altered immune or endocrine function (Banji et al., 2014; He et al., 2022; Meng et al., 2023) have been observed following embryonic exposure to various carbamate insecticides. However, compared to other AChE-inhibiting pesticides, the consequences of embryonic exposure to carbamate insecticides remain relatively unexplored (Pelkonen et al., 2006; Zhang et al., 2022), and recent studies highlight the importance of investigating their developmental effects in greater detail (Seomoon et al., 2025; Tsiaoussis et al., 2018).

Bendiocarb is a carbamate insecticide widely used for public health purposes, mainly in African and Asian countries (Abai et al., 2021; Hien et al., 2020; van den Berg et al., 2021). It has been detected in environmental samples, such as surface water (0.003–0.005 mg/L; WM-Bekele et al., 2024), groundwater (0.181 mg/L; Saeid et al., 2011), as well as in food samples, including honey (0.0033 mg/kg; Stevanović et al., 2024) and vegetables (up to 0.028 mg/kg; Dinede et al., 2023). Moreover, bendiocarb is often involved in the poisoning of wild animals in Poland and Spain, with detected concentrations in the liver of poisoned birds ranging from 1.8 to 7.7 mg/kg (Bertero et al., 2020; Chłopaś-Konowalek et al., 2022; Sell et al., 2022). Based on the World Health Organization's (WHO) recommendation, bendiocarb became an important part of malaria or dengue fever control. It has been ranked among the top ten most extensively used insecticides against human disease vectors in global spraying operations between 2010 and 2019 (van den Berg et al., 2021). The applied dose of bendiocarb during indoor spraying ranges from 100 to 400 mg/m² (Lo et al., 2019; Thawer et al., 2015), which emphasizes the potential of high-dose human or other vertebrate exposure in indoor or occupational context. Human field studies found significant AChE inhibition in the venous blood of workers after these types of spraying operations (Bonsall and Goose, 1986). Additionally, recent studies have highlighted the potential health risks associated with maternal and early-life exposure to bendiocarb, as it can traverse the placental barrier and potentially endanger the developing embryo (Berman et al., 2011; Prahl et al., 2021; Shukla et al., 2022). It has also been demonstrated that increased serum levels of bendiocarb were associated with decreased sperm quality parameters in Chinese males (Chang et al., 2024). Earlier studies have shown that bendiocarb exposure have led to oxidative stress and ultrastructural

changes in various organs (Adiguzel and Kalender, 2020; Apaydin et al., 2017; Bahar and Eraslan, 2023; Holovska et al., 2014; Holovská et al., 2017; Krockova et al., 2012; Küp and Doğanyigit, 2021; Petrovova et al., 2011). Despite these findings, comprehensive evaluation of bendiocarb's developmental effects in vertebrates is still lacking. Our earlier work explored the acute effects of bendiocarb exposure in zebrafish embryos, providing a basis for the present, more detailed toxicological assessment (Gazi et al., 2021). Thus, in this study, we aimed for an extensive evaluation of the sublethal developmental effects of bendiocarb on zebrafish embryos, combining global transcriptomic profiling with functional and morphological assessments to gain deeper insight into the most affected biological processes. The sublethal concentrations applied here induced AChE inhibition levels comparable to those reported in human blood samples following bendiocarb exposure (Bonsall and Goose, 1986).

Due to its advantageous characteristics, the laboratory zebrafish has become a widely utilized model organism across various biological disciplines, particularly in toxicology and ecotoxicology (Horzmann and Freeman, 2018). Additionally, according to EU animal welfare regulations, zebrafish embryos provide opportunities for refinement and replacement, which aligns with the 3Rs principle (Strähle et al., 2012). Zebrafish share many similarities with mammals, including humans, particularly at the molecular and cellular, as well as some tissue and organ levels. Accordingly, their embryos and larvae have emerged as valuable test systems for modeling human diseases and assessing developmental toxicity, which is considered a new approach method (NAM) in chemical testing (Ali et al., 2011; Genge et al., 2016; Hill et al., 2005; Howe et al., 2013). The externally fertilized and almost transparent embryos enable us to study the direct embryonic effects of xenobiotics and still offer the possibility of partial extrapolation to higher vertebrates (Brannen et al., 2010; Nishimura et al., 2016).

In this study, using the zebrafish embryo model, we demonstrated that bendiocarb exposure induced a broad range of sublethal developmental abnormalities, including global morphological changes, impaired locomotor activity and non-associative learning, structural and functional disturbances in the retina and skeletal muscle, notochord damage, and modulation of the innate immune system. All these alterations were accompanied by extensive transcriptional changes, affecting gene sets related to processes ranging from phototransduction to defense mechanisms.

2. Materials and methods

2.1. Zebrafish husbandry and embryo collection

Laboratory AB and transgenic Tg(*mpx:EGFP*) parental (F0) zebrafish lines were maintained at the Institute of Aquaculture and Environmental Safety of the Hungarian University of Agriculture and Life Sciences (Gödöllő, Hungary) in a ZebTech recirculation system (Tecniplast S.p.A., Italy). The Tg(*mpx:EGFP*) line (Mathias et al., 2006) was acquired from the Karlsruhe Institute of Technology (KIT, Karlsruhe, Germany). The zebrafish housing system, equipped with filtration and UV disinfection, maintained water conditions as follows: a temperature of 25.5 ± 0.5 °C, pH at 7.0 ± 0.2 , and a conductivity of 550 ± 50 μ S. Animals were kept in 14/10 h of light/dark cycle. Feeding occurred twice daily with artificial granulated fish feed (Zebrafeed, Sparos Lda.) and twice weekly with *Artemia* nauplii. Spawning occurred in the morning in breeding tanks (Nasiadka and Clark, 2012). Embryos were collected in Petri dishes and sorted under a stereo microscope. For quality control, we investigated the collected eggs under a stereo microscope and selected embryos showing normal cleavage, excluding non-fertilized, coagulated and abnormally dividing ones. The selected embryos were transferred randomly in the control and treatment.

2.2. Bendiocarb exposure and analytical measurements

Zebrafish embryos were exposed to bendiocarb solutions at concentrations of 0.035, 0.2, 0.4, 0.75, and 1.5 mg/L. Zebrafish embryo medium (E3) (5 mM NaCl, 0.18 mM KCl, 0.33 mM CaCl₂, 0.33 mM MgCl₂; pH: 7.2) was used as the solvent and dimethyl sulfoxide (DMSO) served as the vehicle. The final concentration of DMSO in the vehicle and exposed groups was 0.009 %, v/v. The embryos were exposed to bendiocarb from the ~8–16 cell stage until 96 h post-fertilization (hpf), in 100 mm Petri dishes, conducted in technical replicates, with daily renewal of the control and the test solutions (Fig. 1A). Each dish contained 45 mL of either control or test solution, with 30 embryos per dish. For physiological and behavioral analyses, animals were randomly selected and assigned to each experimental group. The chemicals used in the experiments are listed in the Supplementary Material.

Analytical measurements of the highest and lowest bendiocarb solutions were performed by Eurofins Analytical Services Hungary Ltd. Chemical analyses were performed using HPLC–MS/MS (Agilent 1290 HPLC coupled to an Agilent 6490 QQQ) with acetonitrile-based calibration. Deviations from the selected nominal concentrations (0.035 mg/L and 1.5 mg/L) did not exceed ± 20 % (OECD 236 (OECD, 2025)), with measured values of 0.028–0.032 mg/L and 1.2–1.5 mg/L,

respectively. For additional details on the analytical measurements, see the Supplementary Material.

2.3. Morphometric analysis

Morphological differences among the different groups were investigated using landmark-based geometric morphometrics (GMM). Forty zebrafish embryos from two independent experiment were included in each group for the analysis ($n = 40$ /group). Eighteen landmarks (Fig. 1. D) were recorded from zebrafish embryo images using tpsUtil (v1.26.) and tpsDig2 (v2.16.) digital imaging software (Rohlf, 2010a, 2010b). A full Procrustes fit was performed on the landmark coordinates to standardize the datasets, followed by multivariate regression analysis on the logarithm of Centroid Size (logCS) using MorphoJ v1.07a (Klingenberg, 2011). To account for variances arising from allometric growth, statistical analysis was conducted on the residuals of the regression analyses. The standardized datasets were then analyzed using Canonical Variates Analysis (CVA).

2.4. AChE activity measurement

After bendiocarb exposure (at 96 hpf), 20 zebrafish embryos per

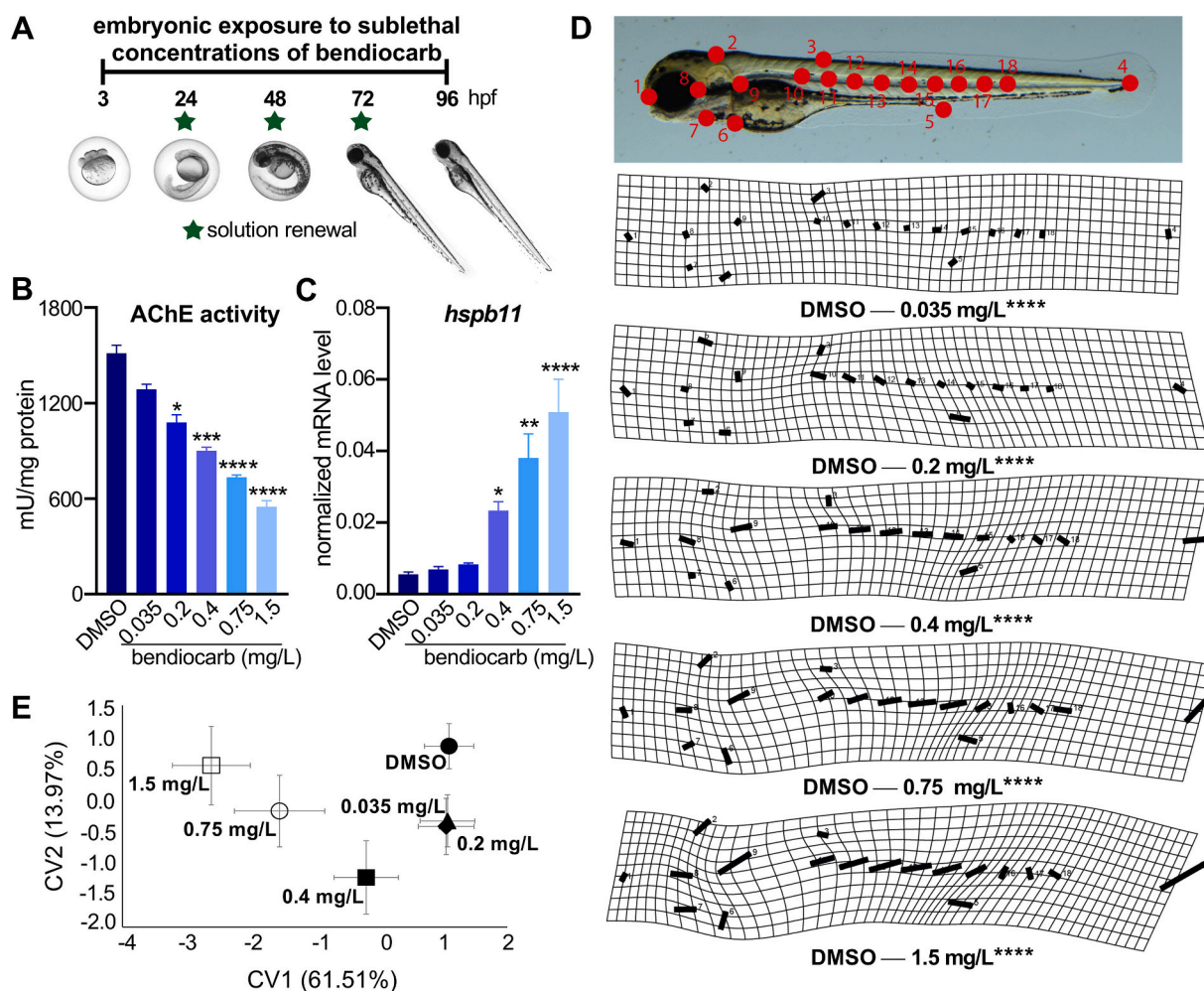


Fig. 1. Effects of sublethal bendiocarb exposure on AChE enzyme activity and 96 hpf zebrafish embryo morphology. (A) Schematic figure of the experimental setup of embryonic bendiocarb-exposure. (B) AChE-inhibitory effect of bendiocarb in the embryos. (C) Expression of the AChE inhibition-sensitive *hspb11* heat shock protein coding gene in the embryos. (D) Representative figures of global morphological alterations resulted from thin plate spline morphometric analysis. Red dots indicate the positions of 18 morphometric landmarks used for the analysis. Black lines on the grids indicate the displacements of the landmarks comparing the bendiocarb-exposed groups to the control (DMSO). Distortions in the grids represent the extent of morphological alterations, which differed significantly in all bendiocarb-exposed groups compared to the DMSO control. (E) CVA plot shows the separation of the groups based on the morphological differences. “*”, “**”, “***”, “****”, and “*****” indicate statistically significant difference at $p < 0.05$, < 0.01 , < 0.001 , and < 0.0001 , respectively, compared to the control (DMSO).

group were collected and pooled together in Eppendorf tubes (three replicates per group per experiment, two subsamples for every replicate, from two independent experiment, $n = 12/\text{group}$) and flash frozen at $-80\text{ }^{\circ}\text{C}$. Samples were homogenized in 100 mM phosphate buffer (containing 100 mM KCl, 1 mM EDTA, 1 mM dithiothreitol (DTT), 0.5 M sucrose, and 0.04 mg/mL aprotinin, $\text{pH} = 7.4$) using a small bead mill (TissueLyser LT, Qiagen, Germantown, MD, USA). Subsequently, homogenates were centrifuged ($6000 \times g$; 3 min; $4\text{ }^{\circ}\text{C}$) and supernatants were stored at $-80\text{ }^{\circ}\text{C}$ until measurement. Enzymatic activities were evaluated in triplicates (technical replicates) at $25\text{ }^{\circ}\text{C}$ using a Thermo Varioskan™ LUX multimode microplate reader (Thermo Fisher Scientific, Waltham, MA, USA).

The determination of AChE activities was carried out according to Ellman's (Ellman et al., 1961) method adapted to microplate (Guilhermino et al., 1996). For additional details on the AChE activity measurement, see the Supplementary Material.

2.5. Behavioral analysis

After bendiocarb exposure, the 96 hpf zebrafish embryos were transferred into sterile 96-well flat-bottom cell culture plates (1 embryo/well, $V_{\text{total}} = 200\text{ }\mu\text{L}/\text{well}$) from two independent experiments with three technical replicates per experiment/group (10 embryos/replicates, $n = 60/\text{group}$). The plates containing the embryos were placed in a ViewPoint ZebraBox instrument. Locomotor activity was continuously monitored under light and dark phases using the default thresholds of the zebrafish behavior analysis system. The high-throughput monitoring system (ViewPoint Behavior Technology) tracked the movement of the embryos during the incubation period of 10 min light - 20 min dark - 10 min light at $25.5 \pm 0.5\text{ }^{\circ}\text{C}$, using the default thresholds of the system. Locomotor activity, i.e., the total distance and duration covered by the embryos in small or large movements, was quantified by the system with a one-minute resolution.

To assess the effects of bendiocarb exposure on learning abilities, 96 hpf zebrafish embryos were tested in three technical replicates (16 embryos/replicates, $n = 48/\text{group}$) in two non-associative learning assays (tactile and visual assays) following bendiocarb treatment. Both assays measure habituation (decreasing response to repeated exposure to harmless stimuli) and dishabituation (restoring response following a different modality stimulus). The assays consist of one pre-stimulus (3 min) and two stimulus periods (3 and 1 min), disrupted by a facilitation event. During the pre-stimulus period, no stimuli are transmitted, while in the stimulus periods, stimuli of modality 'A' are transmitted repeatedly disrupted by a facilitation stimulus of modality 'B'. Habituation is assessed by measuring the distance moved in response to the repeated stimuli in the first stimulus period, while dishabituation is assessed in the second stimulus period in the same way. In the tactile assay, modality 'A' was tactile stimuli transmitted by a Zantiks MWP unit (M100 module) (Zantiks, Cambridge, UK) while modality 'B' was a one-second dark flash, while in the visual assay, it was the other way around. During the pre-stimulus period, no experimental stimuli were delivered; activity in this interval served as the baseline. Tactile and visual assays were done on the same subject in a previously randomized order. The behavior was video recorded by the MWP unit and was analyzed using Noldus Ethovision XT (Noldus). For further details on behavioral evaluation, see the Supplementary Material.

2.6. RNA extraction and RT-qPCR

After bendiocarb exposure, the 96 hpf embryos were transferred into microcentrifuge tubes (30 embryos/group/replicate for RNA sequencing with 3 replicates and 10 embryos/group/replicate for RT-qPCR with 6 replicates) and homogenized in TRIzol Reagent. Total RNA was extracted, reverse-transcribed into cDNA, and gene expression was quantified by qPCR using EvaGreen chemistry on a LightCycler 480 system. For additional details on RT-qPCR, see the Supplementary

Material. Nucleotide sequences of primers are shown in the Supplementary Table S1.

2.7. RNA sequencing and transcriptome analysis

RNA quality was assessed on an Agilent BioAnalyzer, and only samples with $\text{RIN} > 7$ were used for library preparation with the Ultra II RNA Sample Prep Kit for Illumina (New England BioLabs); libraries were sequenced on an Illumina NextSeq 500 (single-end, 75 cycles). Differential expression analysis was performed in DESeq2 with Benjamini-Hochberg FDR correction, considering genes with adjusted $p < 0.10$ as differentially expressed. Raw sequencing data is submitted to the NCBI Sequence Read Archive (SRA) database (PRJNA1181761). For additional details on RNA sequencing and transcriptome analysis, see the Supplementary Material.

2.8. Histology

After a 96-h exposure to bendiocarb, three embryos per group were randomly selected for histological examination. Tissue sectioning and analysis were conducted at the Department of Pathology, University of Veterinary Medicine Budapest. Embryos, fixed in 8 % buffered formaldehyde, were dehydrated in ascending alcohol series followed by xylene impregnation at $56\text{ }^{\circ}\text{C}$. Subsequently, the samples were embedded in Paraplast, and sections were prepared using a microtome. The sections were deparaffinized twice in alternating xylene, followed by washing in a descending alcohol series (absolute ethanol, 96 %, 90 %, 80 %, 70 %, 50 % ethanol) and distilled water. Finally, staining with hematoxylin and eosin was performed for subsequent microscopic examinations. Representative images of sections were selected to show histopathological alterations.

2.9. Evaluation of neutrophil granulocyte number and distribution

We used a neutrophil granulocyte specific transgenic reporter line ($Tg(\text{mpx}:EGFP)$) to evaluate changes in the quantity and distribution of these immune cells in the whole embryos (15 embryos/replicates with 4 replicates/group). Neutrophil counts were measured by flow cytometry, adhering to the protocol outlined by Oehlers et al. (Oehlers et al., 2013). Neutrophil frequency was calculated as the number of EGFP-positive cells per 10^5 cell. For further details on sample preparation and flow cytometry, see the Supplementary Material.

Neutrophil granulocyte distribution in whole embryos and in the notochord region was assessed by imaging the anaesthetized (tricaine mesylate, 168 mg/L, (Matthews and Varga, 2012)) $Tg(\text{mpx}:EGFP)$ embryos under fluorescence microscopes (Leica M205FA equipped with Leica DFC7000T camera and Leica M205FCA equipped with DFC9000GT camera; Leica Application Suite X software (v3.7.2.22383), Leica Microsystems GmbH, Germany). To quantify differences in neutrophil distribution, we counted the number of neutrophil granulocytes within a defined region of interest (ROI), corresponding to the middle trunk area, using the clearly visible notochord as a consistent anatomical landmark across laterally positioned embryos (25 embryos/group). To estimate the three-dimensional position of the EGFP+ cells which were accumulated in the middle region of the trunk, we supplemented the results with dorsal views of embryos from both the control group (DMSO) and the group exposed to the highest concentration of bendiocarb (1.5 mg/L).

2.10. Evaluation of nitric oxide (NO) production and notochord alterations

Production of the stress marker and pro-inflammatory mediator NO in zebrafish embryos was evaluated in vivo by using a cell-permeable fluorescent indicator, DAF FM DA. After bendiocarb exposure, 96 hpf zebrafish embryos (20 embryos/group from two independent

experiments) were incubated for one hour in the dark in sterile 96-well cell culture plates (1 embryo/well) containing 200 μ L 5 μ M DAF FM DA solution per well. Then, the embryos were carefully rinsed in E3 medium and imaged under anaesthesia (tricaine mesylate, 168 mg/L) using fluorescence stereo microscopes (Leica M205FA equipped with Leica DFC7000T camera and Leica M205FCA equipped with DFC9000GT camera; Leica Application Suite X software (v3.7.2.22383), Leica Microsystems GmbH, Germany). We used ImageJ software (v1.53a) to quantify the total area of the lesions and the fluorescence intensities in the notochord. Fluorescence intensities in the notochord were measured after applying a uniform threshold across all images to ensure consistent analysis.

2.11. Tail fin transection

Control and bendiocarb-exposed 96 hpf Tg(mpx:EGFP) zebrafish embryos (20 embryos/group from two independent experiments) were anaesthetized (anaesthesia: tricaine mesylate, 168 mg/L) and the tail fins were transected with a sterile razor blade under a stereo microscope (Leica M205 FA). Particular attention was paid to ensure that the cut was of a similar extent, did not damage the notochord, and left a straight incision line perpendicular to the craniocaudal axis of the embryos. Four hours post injury the embryos were anaesthetized and images were taken from the caudal region under a fluorescence stereo microscope (Leica M205 FA, GFP2 long pass filter). Then, the number of neutrophil granulocytes located at the site of the wound were counted using Leica Application Suite X software (v3.7.2.22383).

2.12. Statistics

Normality of data were tested by the Shapiro-Wilk test. Statistically significant differences ($p < 0.05$) between the control and bendiocarb-exposed groups were assessed using one-way ANOVA and post hoc Dunnett test or Kruskal-Wallis test and post hoc Dunn tests with Bonferroni adjustment for multiplicity. The statistical analysis was performed using GraphPad Prism software (GraphPad Software 8.0.1, La Jolla, CA, USA). Data from the experiments are presented as mean \pm SE. Effect sizes were calculated in R (v4.4.2) and reported as rank-biserial correlation coefficients (r) for Dunn's post hoc comparisons and Hedges' g for Dunnett's multiple comparisons. Data from visual and tactile behavioral assays were analyzed using repeated measure two-way ANOVA with the group, period and group*period interaction terms and animal identities as repeated factors. Effect sizes were reported as eta-squared (η^2). Within each family of pairwise contrasts, p -values were adjusted using the Benjamini–Hochberg FDR procedure ($q = 0.05$). The statistical analysis for this part was performed in R (v4.3.1) statistical environment. Detailed statistical results are available in Supplementary Table S2 (Statistical Results).

2.13. Ethical notes

The European Directive on the Protection of Animals for scientific purposes (2010/63/EU) does not apply to fish embryos before the stage of independent feeding, which begins after 120 h post-fertilization in zebrafish (Strähle et al., 2012). No independently feeding zebrafish larvae or adult animals were involved in our experiments.

3. Results

3.1. Concentration-dependent inhibition of AChE and global morphological changes in zebrafish embryos after bendiocarb exposure

To investigate the sublethal bendiocarb exposure-induced harmful effects during zebrafish embryogenesis, we selected low concentrations based on the 10 % effective concentration ($EC_{10} = 1.06$ mg/L) for severe embryonic deformities (Gazsi et al., 2021), which represents less than 5

% of the estimated LC_{10} value (24.74 mg/L). As shown in Fig. 1A, the zebrafish embryos were exposed to bendiocarb for 96 h with daily test solution renewal. The inhibitory effects of the applied bendiocarb concentrations were confirmed by the measurements of AChE enzyme activity and mRNA expression of the AChE inhibition-sensitive *hspb11* heat shock protein coding gene (Klüver et al., 2011). As expected, the reduction of AChE enzyme activity and induction of *hspb11* mRNA expression proved to be concentration-dependent on bendiocarb in our experimental system (Fig. 1B and C). Since the AChE inhibition induced by the selected concentration range overlapped with the inhibition levels observed in human blood samples (13–29 %) (Bonsall and Goose, 1986), we applied these concentrations for further investigations.

To evaluate the potential morphological effects at the sublethal bendiocarb concentrations, we investigated the embryonic deformities using microscopic analysis. As we expected, the selected low-concentration range did not cause drastic malformations. However, notable differences could be detected in the whole body of the embryos (Supplementary Fig. S1). In addition to a shortened embryonic axis, we observed that bendiocarb exposure also altered the overall shape of the embryonic body. Thus, we performed landmark-based geometric morphometric analysis to quantify these bendiocarb-induced global morphological changes and found a solid concentration-dependent correlation. Our analysis indicated that the morphological changes were not solely due to differences in body size but also involved non-allometric shifts at specific points of the embryonic body. The thin plate spline analysis indicated that these differences between the bendiocarb-treated and the control groups significantly increased with every concentration (Fig. 1D). The morphometric landmarks in the whole embryos showed considerable displacement, with the most notable deformation observed along the middle region of the trunk (Fig. 1D). In addition, changes in the shape of the yolk sac and the head of the embryos were also apparent (Fig. 1D). The overall morphological and non-allometric differences are summarized in the CVA plot (Fig. 1E). The higher the dose, the lower the value on the CV1 axis, which accounts for 61.51 % of the total morphological variance. One unit along this axis represents a morphological difference five times greater than that on the CV2 axis (Fig. 1E). Supplementary Fig. S2 illustrates how the distances in the CVA plot correspond to global alterations in morphometric landmarks, as demonstrated by schematic representations of landmark positions (e.g., at -4 or $+2$ along the CV1-axis).

Taken together, our findings indicate that embryonic exposure to sublethal concentrations of bendiocarb strongly inhibits zebrafish AChE activity and generates complex morphological alterations in the embryos.

3.2. Bendiocarb induces behavioral alterations including impaired response to light-dark transition in zebrafish embryos

In order to investigate the bendiocarb exposure-induced AChE inhibition- and morphological alterations-associated behavioral abnormalities, we applied a light-dark transition-based behavioral test using the ViewPoint ZebraBox high-throughput monitoring system (Fig. 2A). First, we determined the locomotor activity of the bendiocarb-exposed 96 hpf zebrafish embryos conducted in the dark phase of a 10 min light \rightarrow 20 min dark \rightarrow 10 min light incubation period. The locomotor activity showed bendiocarb concentration-dependent reduction compared to the control in the dark phase (Fig. 2B and C). Remarkable differences could be observed in the effects of bendiocarb on small and large movements covered by the embryos. While the large movement activities were decreased above 0.4 mg/L bendiocarb concentrations, the significantly reduced small movement activities were already observed from 0.2 mg/L concentration (Fig. 2D-G). To further characterize the bendiocarb-induced behavioral abnormalities, we aimed to investigate the sensitivity of bendiocarb-exposed embryos to light change. Therefore, we examined the locomotor activity immediately

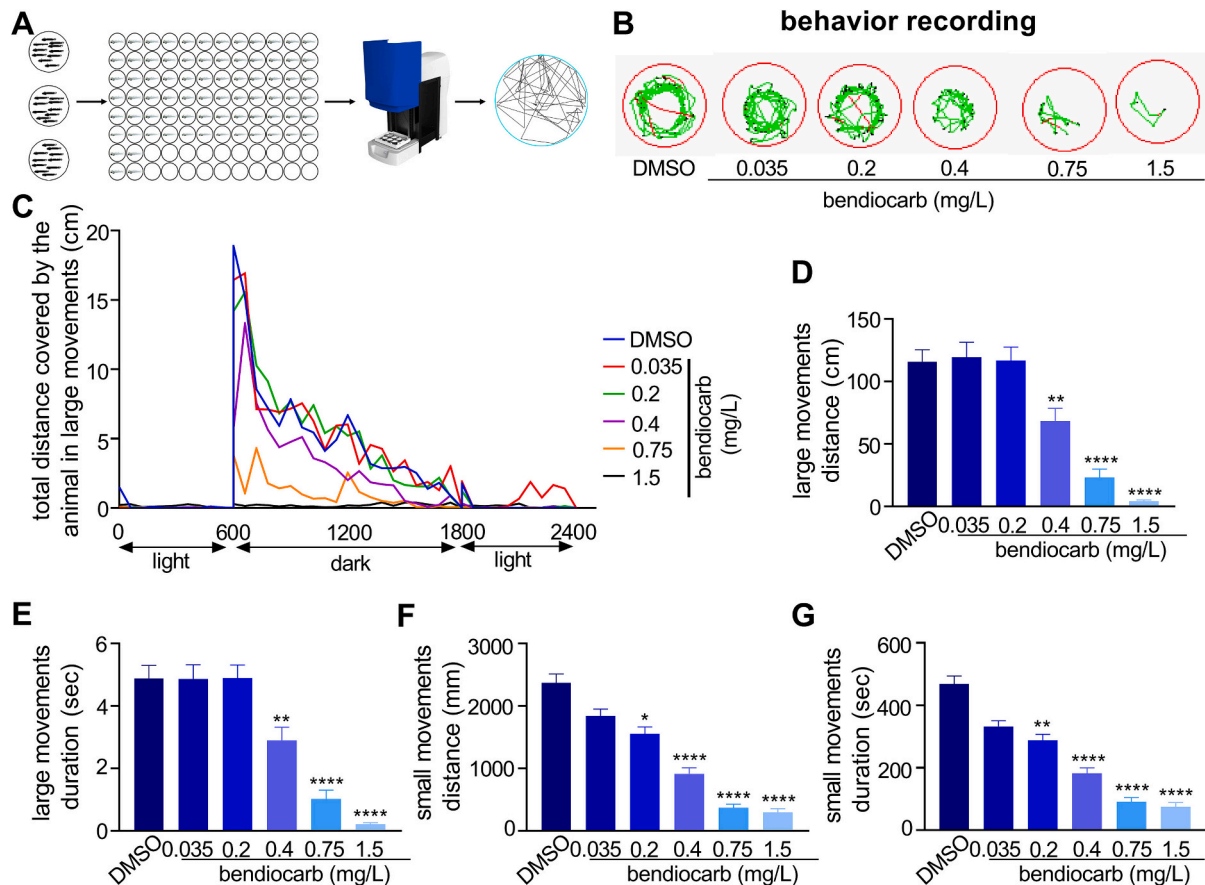


Fig. 2. Effects of sublethal bendiocarb exposure on the locomotor activity and the response to light change in 96 hpf zebrafish embryos. (A) Schematic figure of the experimental setup in the high-throughput zebrafish monitoring system. (B) Visualized examples of movement trajectories (green, red, and black lines) per well (red circles) recorded by the tracking system. (C) The line graph represents the total distance covered by the embryos in large movements per minute during the 10-min light – 20-min dark – 10-min light incubation period. Bar graphs show the total distance (D, F) and duration (E, G) covered by the embryos during the whole 20-min dark phase in large (D, E) and small (F, G) movements. “*”, “****”, “*****”, and “*****” indicate statistically significant difference at $p < 0.05$, < 0.01 , < 0.001 , and < 0.0001 , respectively, compared to the control (DMSO).

after the light-to-dark transition. Figs. 3A and B show that the total distance traveled in large movements significantly decreased from 0.4 mg/L bendiocarb concentration in the first 60 s of the dark period. However, this reduction in locomotor activity was observed only at the two highest applied concentrations in the next 120 s.

Overall, our results suggest that low-concentration bendiocarb exposure leads to the development of vision-based behavioral abnormalities, including diminished sensitivity to the light-to-dark transition and reduced movement activity.

3.3. Bendiocarb diminishes the response integration to visual and tactile stimuli in zebrafish embryos, affecting non-associative learning

To further investigate the bendiocarb-induced behavioral abnormalities and to assess the effects of sublethal bendiocarb exposure on non-associative learning abilities, zebrafish embryos were tested in visual and tactile habituation/dishabituation assays. In both assays repeated measures ANOVA revealed significant time (visual: $F = 22.24$, $p = 9.371e-14$, tactile: $F = 16.55$, $p = 2.937e-10$) and group effects (visual: $F = 10.35$, $p = 1.003e-07$, tactile: $F = 7.24$, $p = 2.139e-05$), as well as time-group interactions (visual: $F = 3.56$, $p = 3.649e-05$, tactile: $F = 16.55$, $p = 2.937e-10$) (Fig. 4A and 5A). Comparisons of 5-s time bins before and after stimuli of the visual assay showed that bendiocarb dose-dependently decreased the number of significant responses to repeated stimuli, indicating a habituation-facilitating effect (Fig. 4A). Performing intra-stimulus comparisons, we detected a significant

decrease in the amplitude of responses in all but the lowest (0.2 mg/L) concentration during the first darkflash stimuli period, indicating concentration- and stimulus-dependent motor effects (Fig. 4B). Intra-group comparisons revealed that bendiocarb exposure changed the behavioral pattern of embryos across the different test periods (Fig. 4C). We detected low stimulus responses in the first stimuli period in the highest doses (0.75 and 1.5 mg/L). However, after tactile stimulus facilitation, locomotor activity was enhanced in these groups, indicating a sensitization effect (Fig. 4C). In the tactile assay (Fig. 5A, B and C), the response amplitudes were significantly lower in all concentrations compared to the control (DMSO) during the facilitation event (Fig. 5B), and responses to sub-threshold tactile stimuli were facilitated by the darkflash stimulus only in the control group (DMSO) and at 0.2 mg/L, indicating that bendiocarb impaired visual facilitation from 0.4 mg/L onward (Fig. 5C).

In summary, different concentrations of bendiocarb affected various forms of non-associative learning, demonstrating both habituation-facilitating and sensitization effects depending on the type of applied stimuli and the stimulus combination. Nevertheless, a negative motor effect was apparent at most concentrations, especially at the highest one.

3.4. Bendiocarb alters gene expression signatures linked to vision, muscle function, immune regulation, regeneration, cell differentiation, and various metabolic processes

To deeply characterize the molecular background of bendiocarb

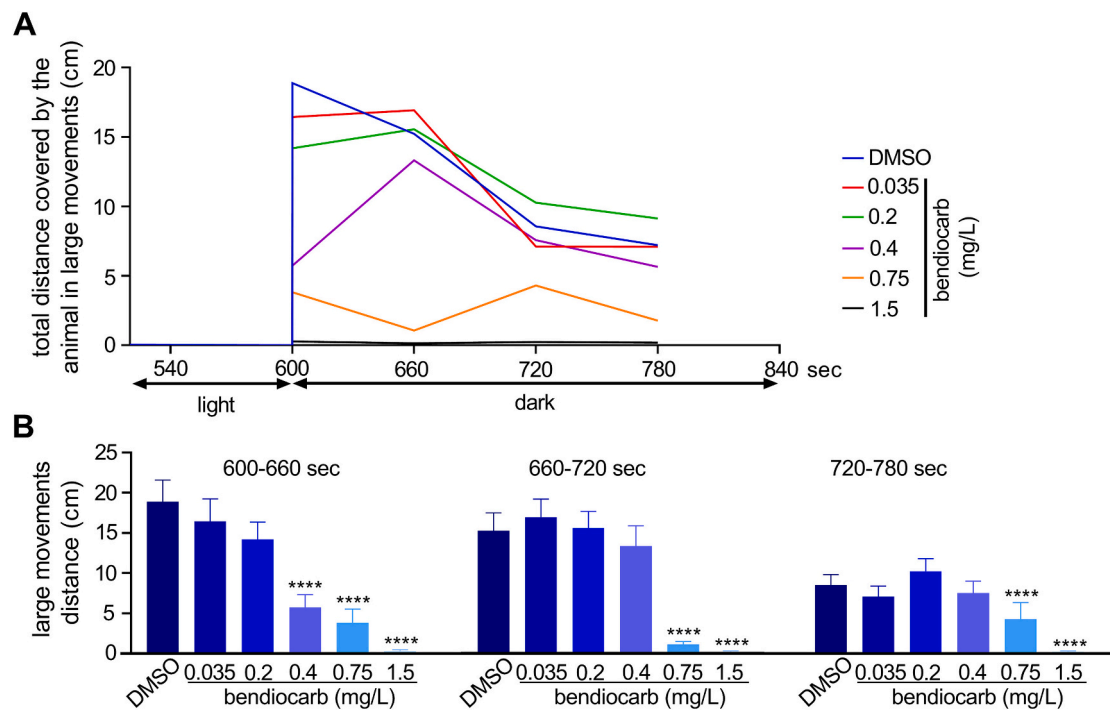


Fig. 3. Effects of sublethal bendiocarb exposure on light change responses in 96 hpf zebrafish embryos. (A) The line graph represents the total distance covered by the embryos in large movements per minute during the light-to-dark transition phase. (B) Bar graphs show the total distance covered by the embryos in large movements during the first 3 min post-transition. “*”, “**”, “***”, and “****” indicate statistically significant difference at $p < 0.05$, < 0.01 , < 0.001 , and < 0.0001 , respectively, compared to the control (DMSO).

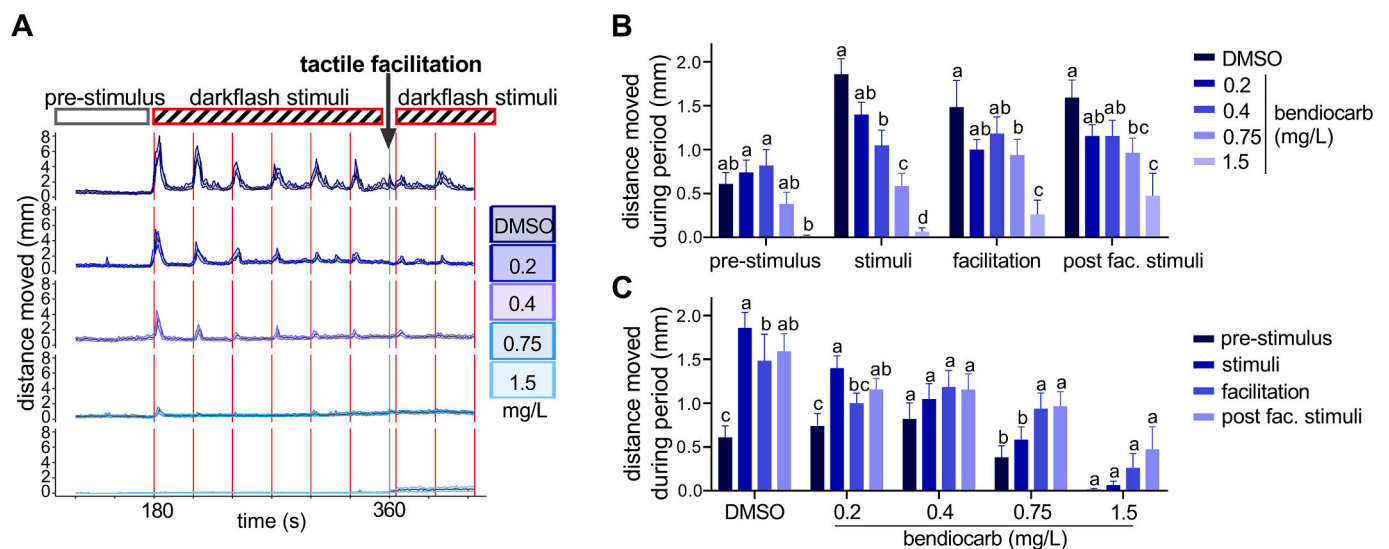


Fig. 4. Effects of sublethal bendiocarb exposure on the locomotor response to visual stimuli with tactile facilitation in 96 hpf zebrafish embryos. (A) Motor responses of the embryos to visual stimuli (darkflash stimulation) before and after tactile facilitation. (B) Intra-stimulus comparisons of locomotor activities. (C) Intra-group comparisons of locomotor activities. Bar graphs show the average distance moved during the distinct periods of the assay. Different letters indicate statistically significant differences ($p < 0.05$) within each type of comparison (intra-stimulus or intra-group).

exposure-induced abnormalities and to potentially identify the affected biological processes, we applied bulk RNA-seq in 96 hpf zebrafish larvae at two different bendiocarb concentrations, including a relatively low, 0.2 mg/L, and the highest applied, 1.5 mg/L. First, we performed principal component analysis (PCA) and found that the distinct treatment conditions were well separated, although the 0.2 mg/L bendiocarb concentration induced less pronounced changes than 1.5 mg/L at the whole transcriptome level compared to the vehicle control (Fig. 6A). Accordingly, our gene expression analysis identified 193 differentially

expressed genes (DEGs; 165 upregulated and 28 downregulated) following 0.2 mg/L bendiocarb exposure compared to DMSO control embryos, while the number of DEGs proved to be 2620 (1743 induced and 877 repressed) at a 1.5 mg/L bendiocarb concentration (Fig. 6B, and Supplementary Table S3). We observed a partial overlap in the up- and downregulated genes between 0.2 and 1.5 mg/L bendiocarb concentrations, including 17 downregulated and 98 upregulated genes at both applied bendiocarb concentrations (Fig. 6C). To identify the biological processes affected by bendiocarb exposure, we performed Gene

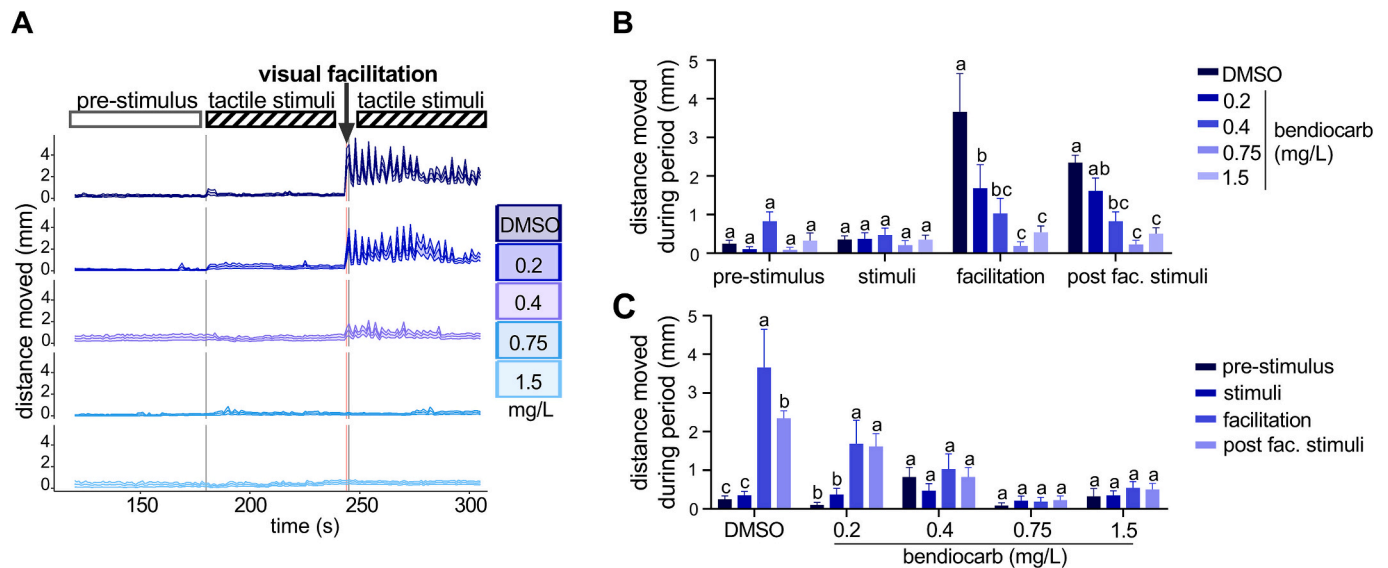


Fig. 5. Effects of sublethal bendiocarb exposure on the locomotor response to tactile stimuli with visual facilitation in 96 hpf zebrafish embryos. (A) Motor responses of the embryos to tactile stimuli before and after visual (darkflash stimulation) facilitation. (B) Intra-stimulus comparisons of locomotor activities. (C) Intra-group comparisons of locomotor activities. Bar graphs show the average distance moved during the distinct periods of the assay. Different letters indicate statistically significant differences ($p < 0.05$) within each type of comparison (intra-stimulus or intra-group).

Ontology (GO) biological process analysis using Cytoscape's ClueGo in each gene subset containing a minimum of 50 genes (Bindea et al., 2009). As shown in Fig. 6D, Supplementary Fig. S3 and Supplementary Table S4, among the up-regulated DEGs, the most prominently enriched GO terms were associated with muscle system, macromolecule and organic substance metabolism, and lipid homeostasis in embryos exposed to 1.5 mg/L bendiocarb. Within these terms, a broad range of genes related to muscle tissue development, muscle cell differentiation, myofibril assembly, sarcomere-, cytoskeleton- and extracellular organization, adhesion, and tissue regeneration were significantly upregulated in the embryos (Supplementary Tables S3 and S4). Additionally, our RNA-seq analysis identified that bendiocarb exposure significantly upregulated three muscle-type nicotinic cholinergic receptor subunit coding genes (*chrna1*, *chrnd*, *chrng*), key components of neuromuscular signal transmission (Supplementary Tables S3 and S4). In addition, innate immune system-related processes, such as defense response and neutrophil granulocyte migration, were also significantly affected (Fig. 6D, Supplementary Fig. S3). These upregulated gene sets contain several members of the complement system, cytokine signaling, toll-like receptors, chemokines, and other key factors involved in cellular and humoral immune responses and inflammation. Furthermore, bendiocarb also induced more than forty genes associated with different regeneration pathways (Supplementary Tables S3 and S4). Next, gene sets related to phosphagen, amine, and pyruvate metabolism, circadian rhythm, and heart morphogenesis were markedly induced at both applied bendiocarb concentrations (Supplementary Fig. S3). Diverse biological processes – e.g., protein depolymerization and cholesterol homeostasis – were affected only by exposure to bendiocarb at a relatively low (0.2 mg/L) concentration (Supplementary Fig. S3). Finally, among the downregulated genes, the most overrepresented categories included chromosome segregation, cell cycle regulation, nervous system development, cytoskeleton organization, visual perception, and sensory organ development-associated terms were the most overrepresented categories in embryos exposed to 1.5 mg/L bendiocarb (Fig. 6E, Supplementary Fig. S3, Supplementary Table S4). Within the downregulated visual perception and sensory organ development-related terms, we found a relatively high proportion of genes with a fundamental role in phototransduction, indicating that bendiocarb affects core pathways in the perception of light (Supplementary Tables S3 and S4).

Taken together, sublethal bendiocarb exposure leads to remarkable

transcriptional changes in zebrafish embryos related to visual perception, muscle formation and function, innate immune system, metabolism and cell division.

3.5. Bendiocarb exposure leads to impaired retinal and muscle-specific gene expression signature and structure

Our results from transcriptome analysis indicated that bendiocarb exposure impairs visual perception and muscle function in zebrafish embryos, and the above-described behavioral abnormalities accompanied these transcriptional changes. To confirm these changes with independent methods, we first studied the vision and retinal development-associated gene set, which showed significantly reduced mRNA expression in embryos exposed to 1.5 mg/L of bendiocarb (Fig. 7A, Supplementary Tables S3 and S4). To investigate the bendiocarb concentration dependency of the diminished vision-associated gene expression signature, we selected *rho* and *opn1mw2*, rhodopsin and opsin coding genes whose functions are crucial in phototransduction, for further RT-qPCR-based validation. Bendiocarb exposure significantly reduced the mRNA expression of both selected genes (Fig. 7B). To further support the observations, we performed histological analysis to study whether the bendiocarb-modified sensory-motor behavior and the altered vision-linked gene expression patterns are associated with structural changes in the eyes of the embryos. As shown in Fig. 7C, degeneration of the retinal layers and substantial vacuolization were observed in histological sections of the eyes in the bendiocarb-exposed (1.5 mg/L) embryos.

Our RNA-seq analysis identified the large number of genes linked to muscle tissue development and function, showing significant induction in bendiocarb-exposed 96 hpf zebrafish embryos (Fig. 8A, Supplementary Tables S3 and S4). To validate these bendiocarb-induced gene expression changes, we selected two genes, *desma* (encoding desmin) and *fn1b* (encoding fibronectin), and we measured their mRNA-expression levels by RT-qPCR. As shown in Fig. 8B, the bendiocarb exposure strongly enhanced their expression in a concentration-dependent manner. Finally, our histological analysis identified severe nuclear and sarcoplasmic lesions in skeletal muscle segments of the bendiocarb-treated embryos (Fig. 8C).

Overall, our findings indicate that bendiocarb exposure impaired the molecular and structural basis of vision and muscle function of the

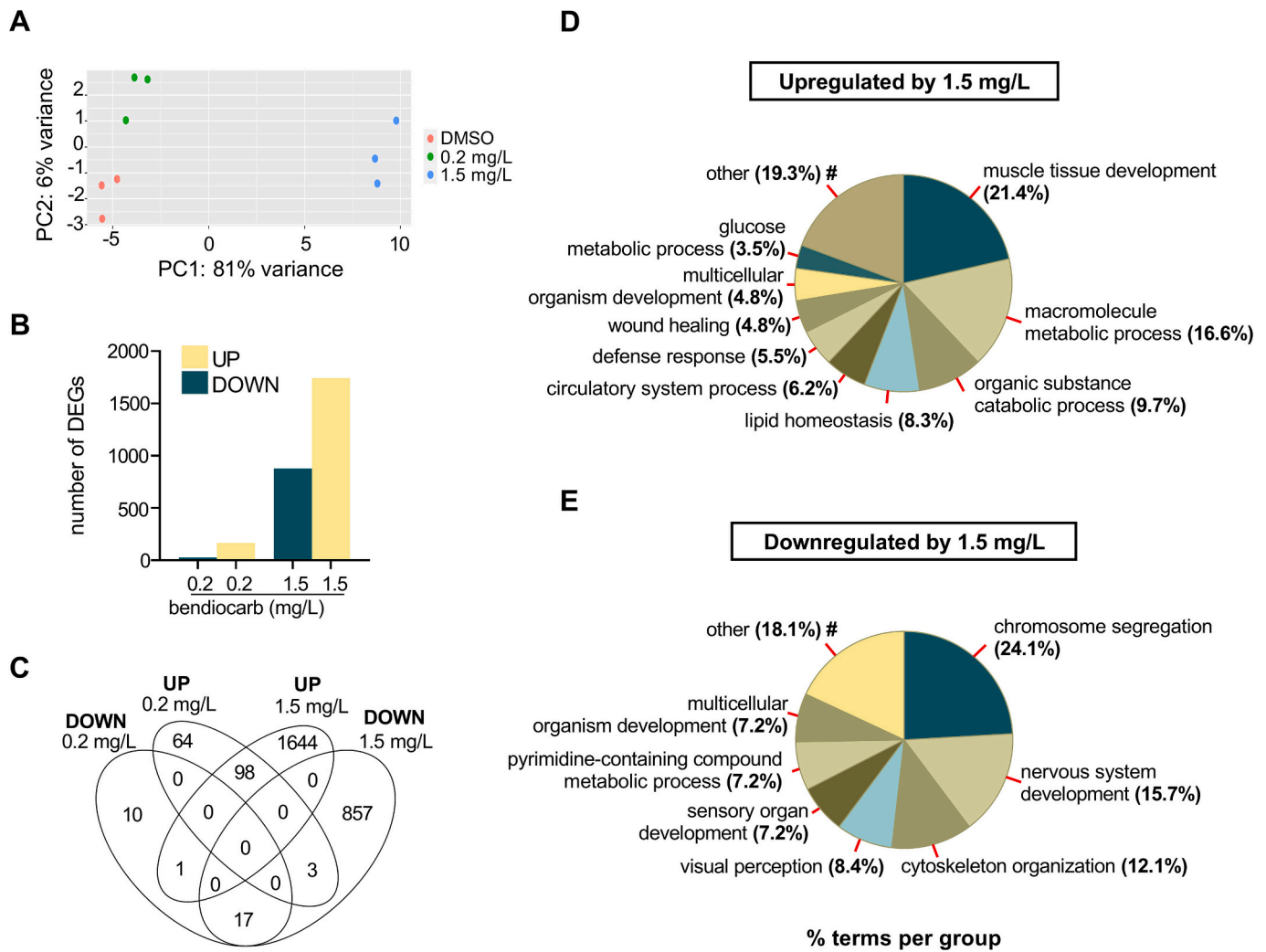


Fig. 6. Global transcriptional alterations triggered by sublethal bendiocarb exposure in 96 hpf zebrafish embryos. (A) Principal component analysis was performed on the RNA-seq data of control (DMSO) and bendiocarb-exposed groups. (B) The number of significantly up- or down-regulated DEGs by bendiocarb. (C) Venn diagram illustrates the distribution and overlap of DEGs between the different experimental groups. Pie charts represent the results of gene ontology enrichment analysis conducted on gene subsets significantly upregulated (D) or downregulated (E) by 1.5 mg/L bendiocarb. Pie charts show the percentage distribution of the significantly enriched terms between the related groups of biological processes. #: detailed results of the affected biological terms are provided in Supplementary Fig. S3 and Supplementary Table S4.

developing embryos, contributing significantly to the observed behavioral abnormalities.

3.6. Bendiocarb exposure triggers notochord disruption and activates defense mechanism

Our morphometric analysis showed that morphological changes along the line of the notochord prominently contributed to the significant whole-body alterations of the bendiocarb-exposed embryos (Fig. 1D, Supplementary Fig. S1). Moreover, our transcriptome analysis revealed that several notochord development and disruption-associated genes were significantly upregulated by bendiocarb (Fig. 9A, Supplementary Tables S3 and S4). Thus, we further characterized the bendiocarb-induced notochord alterations by measuring the expression of the selected notochord development and protection-associated marker genes by RT-qPCR and imaging the notochord area using the Thunder Imaging System (Leica).

On the one hand, we found that bendiocarb exposure could significantly induce the expression of selected notochord development, morphogenesis, and defense mechanism-related genes (Supplementary Tables S3 and S4), including *col8a1a*, *cavin 1b*, and *lox15b*, at mRNA level

in a concentration-dependent manner (Fig. 9B). On the other hand, high-resolution images demonstrated that bendiocarb exposure caused profound structural alterations with severe lesions in the notochord (Fig. 9C). The total area of these lesions increased tremendously at higher concentrations, with a significant difference from 0.4 mg/L (Fig. 9D). To further investigate the extent of notochord damage, we applied a fluorescence-based measurement of NO production, which is a marker of cellular- and tissue-damage-related stressful conditions in the notochord of zebrafish embryos and larvae (Lepiller et al., 2007). We observed that bendiocarb-induced structural alterations in the notochord were accompanied by robust and fragmented fluorescence signals indicating elevated NO level (Fig. 9E). Next, we measured the fluorescence intensities in the whole notochord area to quantify the differences in NO production. The NO level in the notochord showed a concentration-dependent increase with significant differences detected at concentrations above 0.2 mg/L, similar to the trend observed in disrupted areas (Fig. 9F).

Taken together, sublethal bendiocarb exposure altered the expression of notochord development and defense mechanism-related gene sets and exerted significant, NO induction-accompanied structural damage in the notochord of the developing embryos.

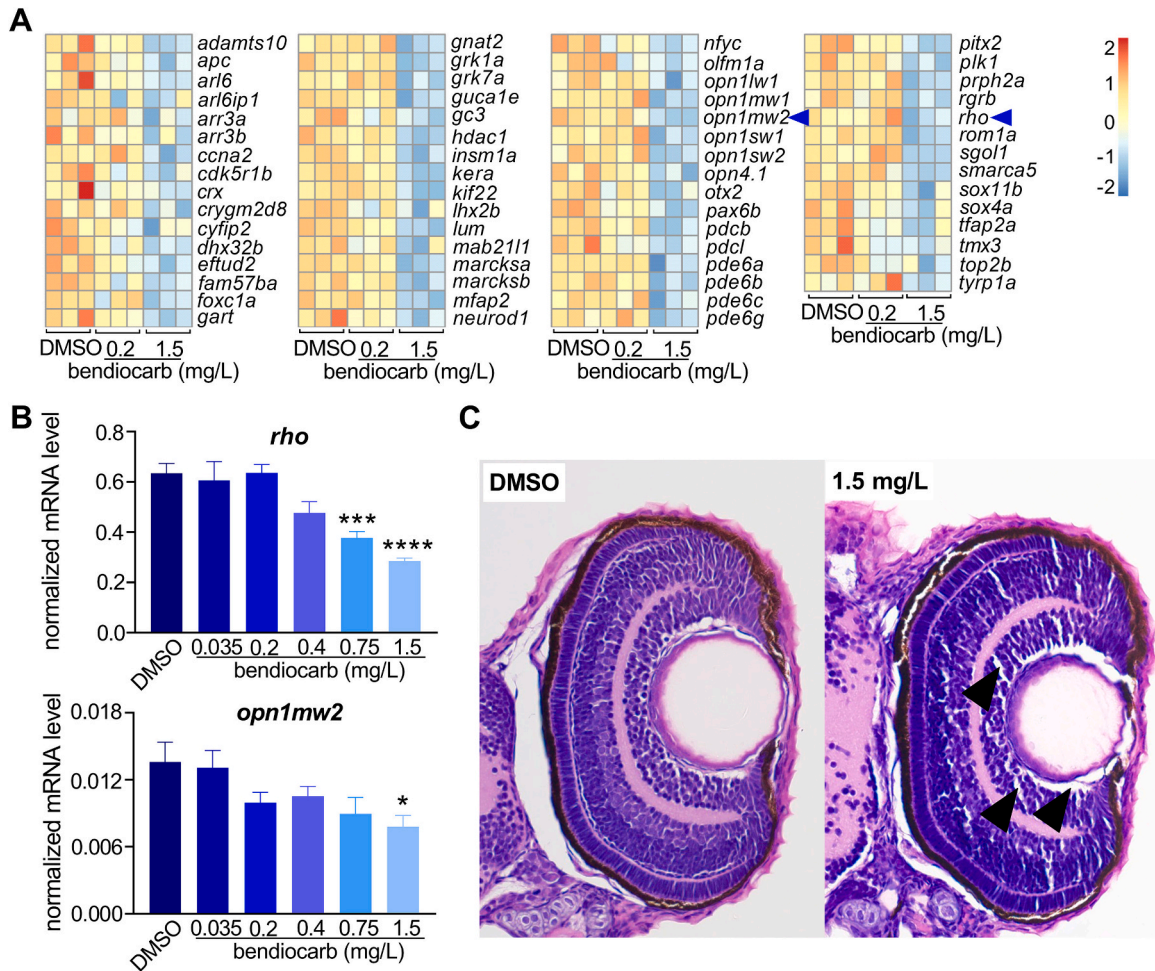


Fig. 7. Bendiocarb exposure represses the expression of visual perception-associated gene sets and disrupts the retinal function and structure of 96 hpf zebrafish embryos. (A) Heat map of the visual system and retinal development and function-related gene set from DEGs identified by our RNA-seq. (B) Expression levels of the selected rhodopsin and opsin coding genes were measured by RT-qPCR. (C) Representative retinal histology (cross-sections) of the 96 hpf zebrafish eyes from the control and bendiocarb-exposed groups. Arrows indicate vacuolization. “***”, “****”, “*****”, and “*****” indicate statistically significant difference at $p < 0.05$, < 0.01 , < 0.001 , and < 0.0001 , respectively, compared to the control (DMSO).

3.7. Bendiocarb exposure alters the distribution and mobilization of neutrophil granulocytes

Our global transcriptome analysis showed that bendiocarb exposure at 1.5 mg/L concentration induced a gene set associated with defense response and neutrophil granulocyte migration and function (Supplementary Fig. S3, Supplementary Tables S3 and S4), raising the possibility of the immunomodulatory effects of bendiocarb. Among the significantly upregulated genes, we found several NF κ B and JAK-STAT signaling pathway members and their target genes, including numerous chemokines, complement factors, and matrix metalloproteinases (Fig. 10A, Supplementary Tables S3 and S4). It has been previously demonstrated that neutrophil granulocyte activation is often associated with xenobiotics- and environmental pollutants-induced inflammation in vertebrates (Pelletier et al., 2001; Xu et al., 2018). Thus, to study the potential inflammatory and immunomodulatory effects of bendiocarb exposure in zebrafish embryos, first, we further characterized the mRNA expression of two neutrophil granulocyte chemoattractant factor genes, *cxcl18b* and *cxcl8b.1*, identified in our RNA-seq experiment using the RT-qPCR method. As shown in Fig. 10B, a concentration-dependent upward trend was observed in their expression above 0.2 mg/L bendiocarb concentration and proved to be significant at concentrations of 0.75 and 1.5 mg/L. Next, we aimed to investigate whether the bendiocarb-induced expression of the measured

chemokines is associated with changes in neutrophil granulocyte number or location in the zebrafish embryos. Therefore, we used a neutrophil granulocyte-specific transgenic Tg(*mpx:EGFP*) zebrafish line and monitored the bendiocarb-induced alterations, evaluating the number and distribution of EGFP positive cells by flow cytometry and fluorescent microscopy (Fig. 10C-E). Significant differences were not detected in the EGFP+ neutrophil granulocyte number (Fig. 10C), but their abnormal distribution was observed in bendiocarb-exposed embryos (Fig. 10D). This altered distribution covered the whole body, particularly the trunk area (Fig. 10D). Thus, we quantified the number of accumulated neutrophils in the middle trunk region, which showed a pronounced increase in the bendiocarb-exposed groups, reaching statistical significance at concentrations above 0.2 mg/L compared to the control (DMSO) (Supplementary Fig. S4A). Additionally, to determine the position of the abnormally distributed neutrophil granulocytes more accurately, we supplemented our results with dorsal views of the embryos. By comparing the lateral and dorsal images of the same embryo, we found that the majority of neutrophil granulocytes accumulating along the longitudinal axis in the trunk have positioned themselves near the surface of the embryonic body (Supplementary Fig. S4B). Next, we were curious whether the notochord disruption is linked to this abnormal neutrophil distribution. Thus, we determined the presence of neutrophil granulocytes in the notochord lesions. According to their location close to the body surface, no considerable neutrophil

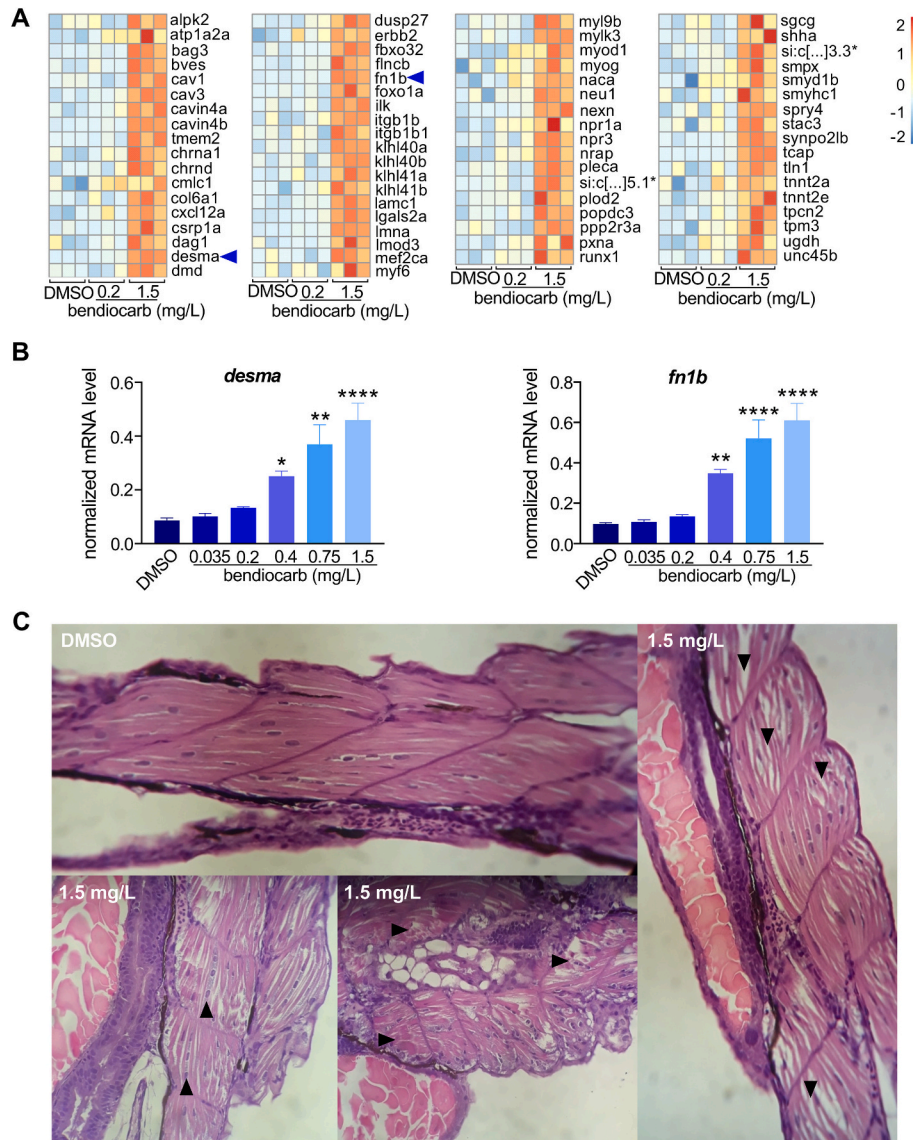


Fig. 8. Bendiocarb exposure induces the expression of muscle function and development-associated gene sets and disrupts the muscle structure of 96 hpf zebrafish embryos. (A) Heat map of muscle function and development-related gene set from DEGs identified by our RNA-seq. (B) Expression levels of the selected desmin and fibronectin coding genes measured by RT-qPCR. (C) Representative histological sections of the 96 hpf zebrafish myotomes from the control and bendiocarb-exposed groups. Arrows indicate multinucleated myoblasts with euchromatic nuclei (▲); discoid degeneration (▶); intercellular edema (▼). “*”, “**”, “***”, and “****” indicate statistically significant difference at $p < 0.05$, < 0.01 , < 0.001 , and < 0.0001 , respectively, compared to the control (DMSO).

accumulation was detected overlapping with the notochord lesions on the high-resolution images (Fig. 10E).

Finally, we aimed to explore whether bendiocarb-induced changes in the distribution of neutrophil granulocytes can influence their mobilization following local tissue injury. For this investigation, we applied a widely used tail fin transection model and determined the recruited neutrophil granulocyte number at the site of injury four hours after the transection (Fig. 11A). As shown in Fig. 11B and C, a significant, concentration-dependent reduction of neutrophil granulocyte recruitment was detected four hours after the wounding.

Overall, our findings suggest that bendiocarb exposure exerts immunomodulatory effects in zebrafish embryos, affecting immune response-associated gene networks, and specifically altering the distribution of neutrophil granulocytes and the mobilization of these innate immune cells in response to a local injury.

4. Discussion

4.1. Effects on morphology, muscle system and notochord

Embryotoxic or teratogenic effects of carbamate and organophosphate insecticides have frequently been associated with impaired growth in vertebrates (Banji et al., 2014; Tsiaoussis et al., 2018; Zhang et al., 2022), consistent with our results. However, the underlying mechanisms remain poorly understood (Tsiaoussis et al., 2018). In contrast to chicken embryo studies where sublethal bendiocarb exposure did not result in major malformations (Petrovova et al., 2012, 2010b, 2009), we detected broad range of pronounced developmental effects in zebrafish embryos. Bendiocarb exposure not only reduced body length but also induced widespread non-allometric morphological alterations affecting the entire embryonic body, including the trunk, the yolk sac, and the head. These morphological changes were accompanied by histopathological evidence of muscle system alterations and impaired notochord development and structure. At the transcriptional level, we

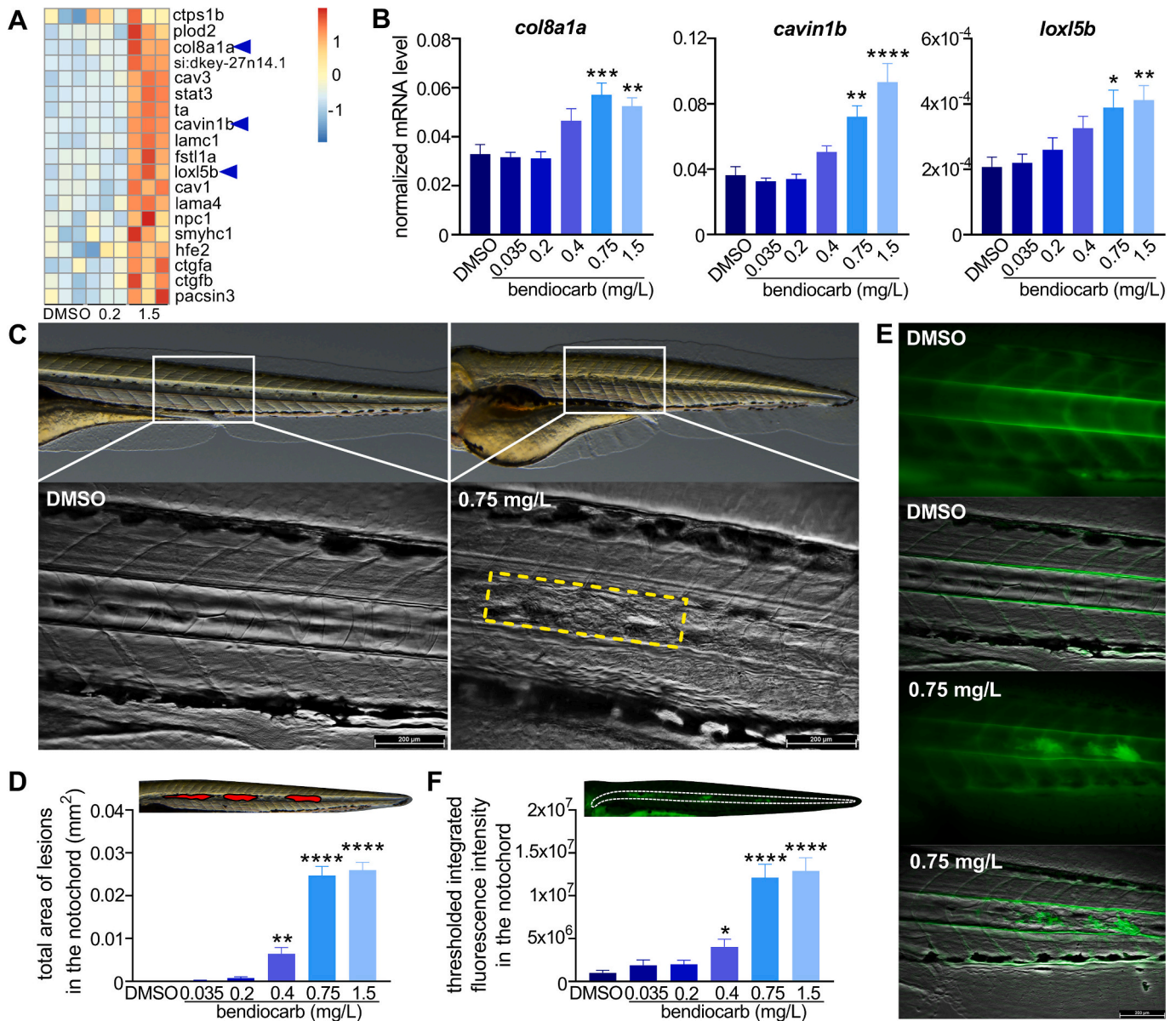


Fig. 9. Bendiocarb exposure induced notochord disruption in 96 hpf zebrafish embryos. (A) Heat map of notochord development and protection-related gene set from DEGs identified by our RNA-seq. (B) Expression levels of the selected notochord development and protection-associated genes measured by RT-qPCR. (C) Representative images (Thunder Imaging, Leica) taken from the notochord region of the control (DMSO) and exposed (0.75 mg/L) embryos. A yellow rectangle with dashed lines indicates an extensive lesion in the notochord. (D) Total area of lesions in the notochord. (E) Representative images (Thunder Imaging, Leica) showing NO production in the notochord of control (DMSO) and exposed (0.75 mg/L) embryos after DAF-FM-DA labeling. (F) NO production in the notochord of the control (DMSO) and exposed embryos quantified as threshold integrated fluorescence. **, ***, ****, and ***** indicate statistically significant difference at $p < 0.05$, < 0.01 , < 0.001 , and < 0.0001 , respectively, compared to the control (DMSO).

detected significant induction of gene sets related to muscle development and structure, neuro-muscular function, and notochord damage-associated defense response. At the same time, processes associated with neurodevelopment, axon projection and cell proliferation were downregulated. The concentration-dependent AChE inhibition observed in our study likely contributes to these morphological and developmental alterations, in line with previous studies linking AChE disruption to muscle, neural, and notochord defects in developing vertebrates (Behra et al., 2002; Chatonnet et al., 2005; Fischer et al., 2015). In line with this, elevated neuromuscular activity has been shown to cause body-axis shortening and muscle degeneration (Lefebvre et al., 2004) and notochord deformation has been linked to contraction-driven mechanical stress (Haendel et al., 2004; Stehr et al., 2006; Che et al., 2023). Similarly, the AChE-inhibitor oxamyl induced body shortening and

defective notochord development (An et al., 2023b), which share common features with the alterations observed in this study. It is well established that inadequate notochord structure and development, muscle dysfunction and impaired neurodevelopment strongly influence vertebrate morphogenesis (Blagden et al., 1997; Ellis et al., 2013; Nayak et al., 2025; Ochi and Westerfield, 2007; Ornoy, 2006; Schwartz et al., 2012). However, the causal links between AChE inhibition-related neuromuscular and notochord alterations and the observed developmental abnormalities remain to be fully elucidated. Some of the observed alterations in this study may also involve non-cholinergic mechanisms, as suggested by dysregulated energy metabolism and cell-cycle pathways. Carbamates, including bendiocarb, can inhibit carboxylesterases, leading to lipid metabolism disturbances through non-cholinergic toxicity (Howell et al., 2018; Liao et al., 2025).

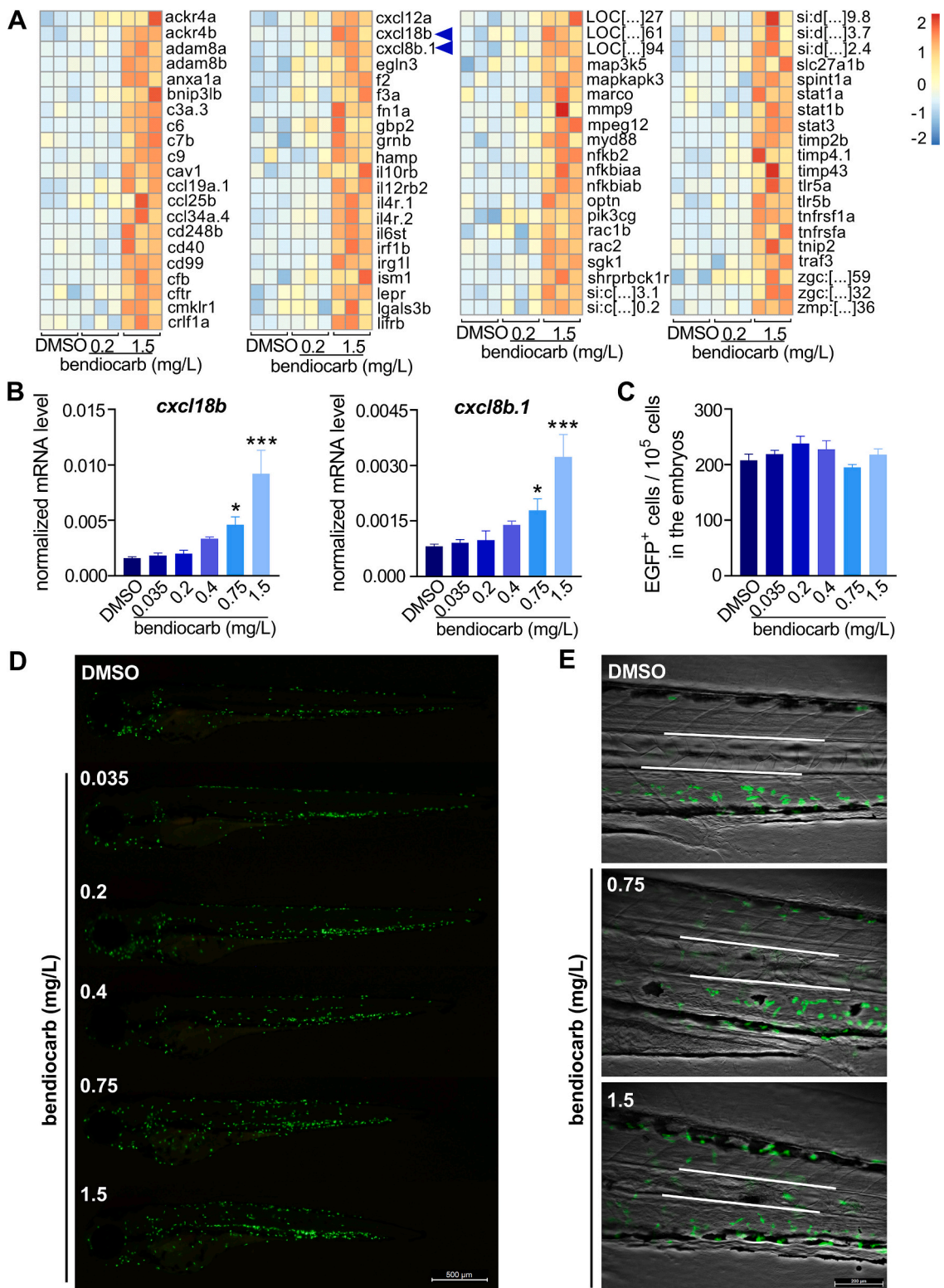


Fig. 10. Effects of sublethal bendiocarb exposure on the innate immune system of 96 hpf zebrafish embryos. (A) Heat map of immune system and defense response-related gene set from DEGs identified by our RNA-seq. (B) Expression levels of the selected neutrophil granulocyte chemotaxis-associated genes measured by RT-qPCR. (C) Frequency of EGFP-positive cells in the whole embryos. (D) Representative images of Tg(mpx:EGFP) embryos showing different neutrophil distribution in the control (DMSO) and exposed groups. (E) Merged, high-resolution images (Thunder Imaging, Leica) taken from the trunk in the middle area of the embryos. White lines indicate the margins of the notochord. “*”, “**”, “***”, and “****” indicate statistically significant difference at $p < 0.05$, < 0.01 , < 0.001 , and < 0.0001 , respectively, compared to the control (DMSO).

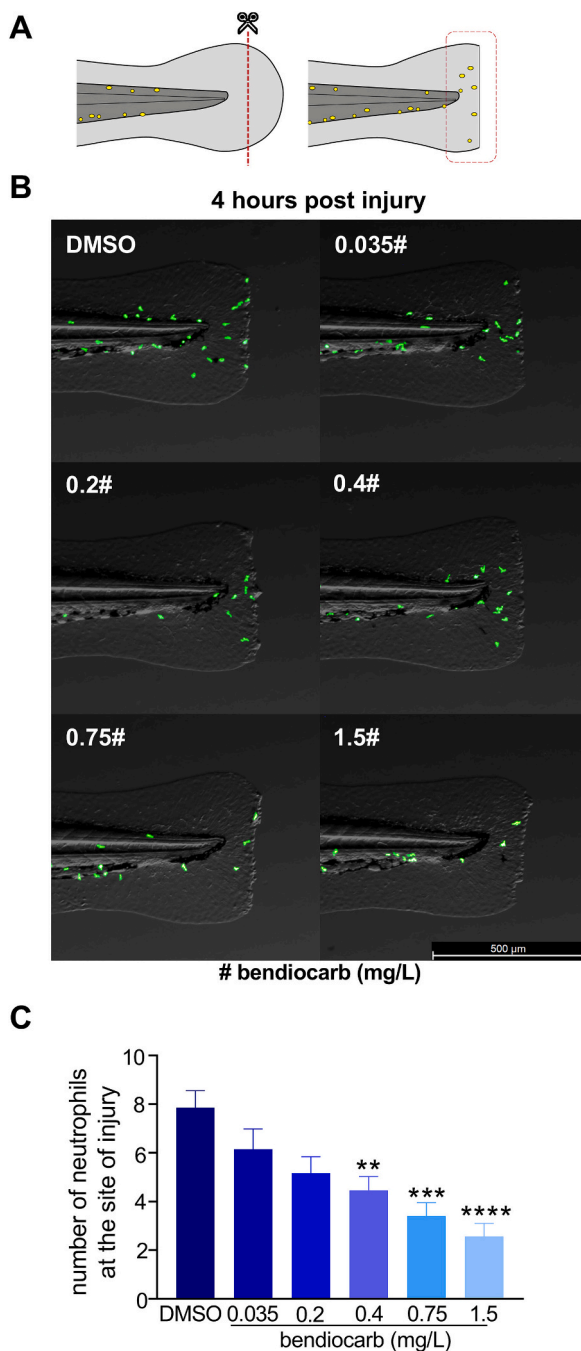


Fig. 11. Bendiocarb exposure impairs neutrophil response to a local injury in 96 hpf zebrafish embryos. (A) Schematic figure of the tail fin transection model marking the site of the injury (area with dashed line). (B) Representative images from the caudal region of Tg(mpx:EGFP) embryos at 4 h post transection. (C) Number of neutrophil granulocytes at the site of injury at 4 h post transection. “**”, “***”, “****”, and “*****” indicate statistically significant difference at $p < 0.05$, < 0.01 , < 0.001 , and < 0.0001 , respectively, compared to the control (DMSO).

Perturbation of energy metabolism during embryogenesis can lead to congenital malformations and adult-onset diseases as well (Illsinger and Das, 2010; Levin, 2006). Additionally, we found that sublethal bendiocarb exposure downregulated several key developmental regulator genes (e.g., *apc*, *cyp26A1*, *hdac1*, *notch1a*, *notch3*, *wnt5b*, *otx2b*, *pax6b*, *tfap2a*, *kif14*, *cenpf*, and *pitx2*), many of which are essential for morphogenesis and organ function (Abu-Abed et al., 2002; Brunmeir et al., 2009; Guo and Xing, 2022; Kuraguchi et al., 2006; Li and Cornell,

2007; Penton et al., 2012; Zhou et al., 2019). These molecular findings provide mechanistic support for the developmental alterations we observed.

4.2. Behavioral and visual effects

The muscular, neurological, and morphological alterations prompted further investigation into the behavioral consequences of bendiocarb exposure. We found significant impairments in locomotor activity and in response to visual and tactile stimuli in the zebrafish embryos. In addition to a general reduction in motor activity, interestingly, we observed both habituation-facilitating and sensitizing effects, suggesting altered non-associative learning capacity. Such multifaceted behavioral alterations are consistent with previous reports that anti-AChE pesticides can induce diverse outcomes in vertebrates, including hypo- or hyperactivity, anxiety-like behavior, and impaired learning and memory (Cao et al., 2019; Correia et al., 2019; Kamboj and Sandhir, 2007; Lee et al., 2015; Liu et al., 2020a; Zhang et al., 2018). Moreover, impaired motor development has been documented following fetal exposure to the carbamate propoxur, a structural analog of bendiocarb (Ostrea et al., 2012). The gradual decline in responsiveness to repeated visual stimuli, as well as overreactions following tactile facilitation, indicates dysfunctions across the visual detection, signal transmission, sensorimotor integration, and neuromuscular execution in the bendiocarb-exposed groups. These behavioral alterations are consistent with impaired retinal development and function, supported by histopathological findings and transcriptomic evidence of phototransduction pathway downregulation. Notably, opsin and rhodopsin mRNA levels showed a concentration-dependent decrease, as confirmed by qPCR. These findings provide novel insights into the sensory-motor disruptions associated with carbamate exposure during early vertebrate development. Previous studies have highlighted the importance of AChE in retinal integrity, with knockout leading to degeneration (Bytyqi et al., 2004) and excessive expression linked to gliosis and aberrant neovascularization (Liu et al., 2020b). In human populations, organophosphate exposure has been linked to ocular degeneration and visual impairments (Dahanayake et al., 2020; Montgomery et al., 2005). However, the effects of carbamates on retina development and visual function during embryogenesis remain poorly characterized. Our findings extend this knowledge by demonstrating that bendiocarb induces structural eye damage and suppresses phototransduction-related genes in zebrafish embryos. This retinal disruption may substantially contribute to the observed visual system-related behavioral abnormalities, although the relative contributions of AChE inhibition and potential non-cholinergic mechanisms require further elucidation.

4.3. Effects on innate immune system

The immunological consequences of bendiocarb exposure remain poorly understood, with most studies focusing on the adaptive immune system, such as altered lymphoid tissues in rabbits (Petrovova et al., 2011, 2010a) and reduced regulatory T-cell numbers in human infants (Prah et al., 2021). Our study demonstrated that the developing innate immune system is also a significant target of bendiocarb. Sublethal bendiocarb exposure induced the upregulation of inflammation-related gene signatures, including Toll-like receptor signaling, prostaglandin metabolism, JAK/STAT signaling, granulocyte recruitment, and matrix remodeling. This altered gene expression signature, including the elevated neutrophil granulocyte chemoattractant factors *cxcl18b* and *cxcl8b.1*, was associated with abnormal neutrophil granulocyte distribution without a change in their number in the bendiocarb-exposed embryos. Moreover, we detected that the neutrophil granulocyte migration was diminished to the injury site after tail fin transection in bendiocarb-exposed embryos. Based on these results, we hypothesize that the altered neutrophil signaling pathways and their abnormal accumulation may contribute to the impaired migratory capacity of

these cells in response to tissue damage. Comparable alterations in neutrophil distribution and migration have been described following other xenobiotic exposures in zebrafish, such as aflatoxin B1 (Ivánovics et al., 2021), famoxadone-cymoxanil and cyhalofop-butyl (Cheng et al., 2021, 2020), and various organic pollutants and metals (Xie et al., 2021; Xu et al., 2018). Overall, our results indicate that the carbamate insecticide bendiocarb induces inflammation in the developing embryo and impairs tissue damage-associated innate immune response. These results expand current understanding of carbamate embryotoxicity by revealing that the innate immune system is a previously less recognized target during early vertebrate development. However, further functional assessments are required to achieve a more detailed immunotoxicological evaluation of bendiocarb. Finally, while AChE inhibition has been linked to both anti-inflammatory and pro-inflammatory effects (Banks and Lein, 2012; Benfante et al., 2021), it remains to be elucidated to what extent the immunological alterations we observed after bendiocarb exposure rely on cholinergic mechanisms.

5. Study limitations

The high percentage of orthologs among protein-coding genes and the similarities at cellular, tissue, and organ levels allow for a certain degree of extrapolation from zebrafish to higher vertebrates, including humans (Brannen et al., 2010; Howe et al., 2013). However, the zebrafish embryo model has limitations, primarily due to the lack of a mother-placenta-embryo relationship. Although the applied concentrations in this study induced AChE inhibition overlapping with inhibition levels measured in human blood, and certain environmental samples overlapped with (0.181 mg/L; Saeid et al., 2011) or were close to (0.028 mg/kg; Dinede et al., 2023) our applied range, real-world exposure scenarios may differ from the controlled concentrations applied in the laboratory. Furthermore, our investigation was restricted to the embryonic developmental window; therefore, potential juvenile- and adult-onset effects of bendiocarb exposure warrant further investigation. In addition, only three embryos per group were processed for histological evaluation, which limits the strength of these observations; nevertheless, the results were consistent with the molecular and morphological findings. Finally, although our transcriptional profiling results align with functional and morphological assessments, incorporating protein-level analysis in future studies could further enhance the understanding of bendiocarb-induced developmental toxicity.

6. Conclusion

Our toxicological evaluation of sublethal bendiocarb exposure in zebrafish embryos revealed complex morphological, behavioral, histological, transcriptional, and immunological alterations. The observed effects are associated with AChE inhibition, as supported by previous reports linking AChE inhibition to neuromuscular dysfunction and related morphological changes. At the same time, bendiocarb perturbed numerous non-cholinergic pathways (such as energy metabolism and gene networks governing cell proliferation and differentiation), indicating that multiple mechanisms underlie its embryotoxicity. Given that AChE inhibition by carbamate insecticides is reversible, future studies should assess which biological effects are transient and which represent persistent or long-term consequences. While the prevention of insect-borne human diseases remains essential, the relatively high application rate of bendiocarb during indoor spraying operations highlight the importance of considering potential developmental effects in the light of our findings. Taken together, our results provide a comparative framework for evaluating the embryotoxicity of carbamate insecticides and offer valuable insights into the potential developmental impacts in higher vertebrates. The adverse outcomes observed in our zebrafish model underscore the need for particular caution regarding maternal carbamate exposure and highlight the importance of complementary studies in mammalian systems, as well as the development of

insecticides with higher margin of safety.

Supplementary data to this article can be found online at <https://doi.org/10.1016/j.cbpc.2025.110368>.

CRediT authorship contribution statement

Bence Ivánovics: Writing – review & editing, Writing – original draft, Visualization, Methodology, Investigation, Data curation, Conceptualization. **Gyöngyi Gazi:** Writing – original draft, Visualization, Methodology, Investigation, Conceptualization. **Zoltán K. Varga:** Writing – review & editing, Visualization, Methodology, Investigation, Data curation. **Ádám Staszny:** Visualization, Software, Methodology, Data curation. **Eszter Váradi:** Software, Methodology, Data curation. **Zsófia Varga:** Methodology, Investigation. **András Ács:** Methodology, Investigation, Data curation. **Márta Tóth:** Methodology, Investigation, Data curation. **Apolka Domokos:** Methodology, Investigation. **Márta Reining:** Methodology, Investigation. **Erna Vásárhelyi:** Methodology, Investigation. **Szilárd Póliska:** Software, Methodology, Data curation. **Róbert Kovács:** Methodology, Investigation, Conceptualization. **Ferenc Baska:** Methodology, Investigation. **Zoltán Filep:** Validation. **Attila Bácsi:** Writing – review & editing. **Julianna Kobolák:** Writing – review & editing, Project administration, Funding acquisition. **Béla Urbányi:** Resources, Project administration, Funding acquisition. **István Szabó:** Resources, Project administration, Funding acquisition. **Tamás Müller:** Resources, Project administration, Funding acquisition. **Zsolt Csenki-Bakos:** Writing – review & editing, Supervision, Funding acquisition, Conceptualization. **Zsolt Czimmerer:** Writing – review & editing, Writing – original draft, Visualization, Supervision, Methodology, Funding acquisition, Conceptualization.

Funding

Project no.2020–1.1.2-PIACI-KFI-2021-00239 has been implemented with the support provided by the Ministry of Innovation and Technology of Hungary from the National Research, Development and Innovation Fund, financed under the PIACI KFI funding scheme. This research was also supported by the Ministry of Innovation and Technology within the framework of the Thematic Excellence Programme 2021, National Defense and Security sub-programme (TKP2021-NVA-22) and by the National Research Development and Innovation Office of Hungary (NKFI ADVANCED - 150916). B.I. was supported by the EKÖP-MATE/2024/25/K (EKÖP-24-VI/MATE-18) University Research Scholarship Programme of the Ministry for Culture and Innovation from the source of the National Research, Development and Innovation Fund. S.P. was supported by the project TKP2021-NKTA-34, which has been implemented with the support provided by the Ministry of Culture and Innovation of Hungary from the National Research, Development and Innovation Fund, financed under the TKP2021-NKTA funding scheme. Authors (B.U. I-S and T.M.) gratefully acknowledge the support of the Flagship Research Groups Programme and the Research Excellence Programme (Z.C.-B.) of the Hungarian University of Agriculture and Life Sciences. ZC is supported by the New National Excellence Program of the Ministry for Innovation and Technology (ÚNKP-22-5 – SZTE-549) and by the János Bolyai Research Scholarship of the Hungarian Academy of Sciences BO/00594/22/8.

Declaration of competing interest

The authors declare that they have no known competing financial interests or personal relationships that could have appeared to influence the work reported in this paper.

Acknowledgements

The Authors kindly acknowledge Anita Rác for managing zebrafish maintenance and ensuring proper laboratory conditions for the

behavioral investigations.

Data availability

Raw sequencing data is submitted to the NCBI Sequence Read Archive (SRA) database (PRJNA1181761). Additional data will be made available on request.

References

- Abai, M.R., Vatandoost, H., Dorzadeh, H., Shayeghi, M., Hanafi-bojd, A.A., Raeisi, A., 2021. Bioefficacy of bendiocarb WP80 in vector-borne and zoonotic diseases areas in borderline of Iran and Pakistan. *Toxicol. Res. (Camb)*. 10, 868–874.
- Abu-Abed, S., MacLean, G., Fraulob, V., Chambon, P., Petkovich, M., Dolle, P., 2002. Differential expression of the retinoic acid-metabolizing enzymes CYP26A1 and CYP26B1 during murine organogenesis. *Mech. Dev.* 110, 173–177.
- Addissie, Y.A., Kruszka, P., Troia, A., Wong, Z.C., Everson, J.L., Kozel, B.A., Lipinski, R.J., Malecki, K.M.C., Muenke, M., 2020. Prenatal exposure to pesticides and risk for holoprosencephaly: a case-control study. *Environ. Heal. A Glob. Access Sci. Source* 19, 1–13. <https://doi.org/10.1186/s12940-020-00611-z>.
- Adiguzel, C., Kalender, Y., 2020. Bendiocarb-induced nephrotoxicity in rats and the protective role of vitamins C and E. *Environ. Sci. Pollut. Res.* 27, 6449–6458. <https://doi.org/10.1007/s11356-019-07260-x>.
- Ait-Bali, Y., Ba-M'hamed, S., Bennis, M., 2016. Prenatal paraquat exposure induces neurobehavioral and cognitive changes in mice offspring. *Environ. Toxicol. Pharmacol.* 48, 53–62. <https://doi.org/10.1016/j.etap.2016.10.008>.
- Ali, S., van Mil, H.G.J., Richardson, M.K., 2011. Large-scale assessment of the zebrafish embryo as a possible predictive model in toxicity testing. *PLoS One* 6, e21076. <https://doi.org/10.1371/journal.pone.0021076>.
- Amstislavsky, S.Y., Kizilova, E.A., Eroschenko, V.P., 2003. Preimplantation mouse embryo development as a target of the pesticide methoxychlor. *Reprod. Toxicol.* 17, 359. [https://doi.org/10.1016/S0890-6238\(03\)00043-1](https://doi.org/10.1016/S0890-6238(03)00043-1).
- An, G., Hong, T., Park, H., Lim, W., Song, G., 2023a. Oxamyl exerts developmental toxic effects in zebrafish by disrupting the mitochondrial electron transport chain and modulating PI3K/Akt and p38 Mapk signaling. *Sci. Total Environ.* 859. <https://doi.org/10.1016/j.scitotenv.2022.160458>.
- An, G., Hong, T., Park, H., Lim, W., Song, G., 2023b. Oxamyl exerts developmental toxic effects in zebrafish by disrupting the mitochondrial electron transport chain and modulating PI3K/Akt and p38 Mapk signaling. *Sci. Total Environ.* 859, 160458. <https://doi.org/10.1016/j.scitotenv.2022.160458>.
- Apaydin, F.G., Baş, H., Kalender, S., Kalender, Y., 2017. Bendiocarb induced histopathological and biochemical alterations in rat liver and preventive role of vitamins C and E. *Environ. Toxicol. Pharmacol.* 49, 148–155. <https://doi.org/10.1016/j.etap.2016.11.018>.
- Bahar, O., Eraslan, G., 2023. Investigation of the efficacy of diosmin against organ damage caused by bendiocarb in male Wistar albino rats. *Environ. Sci. Pollut. Res.* 30, 55826–55845. <https://doi.org/10.1007/s11356-023-26105-2>.
- Banji, D., Banji, O.J.F., Ragini, M., Annamalai, A.R., 2014. Carbosulfen exposure during embryonic period can cause developmental disability in rats. *Environ. Toxicol. Pharmacol.* 38, 230–238. <https://doi.org/10.1016/j.etap.2014.05.009>.
- Banks, C.N., Lein, P.J., 2012. A review of experimental evidence linking neurotoxic organophosphorus compounds and inflammation. *Neurotoxicology* 33, 575–584. <https://doi.org/10.1016/j.neuro.2012.02.002>.
- Behra, M., Cousin, X., Bertrand, C., Vonesch, J.L., Biellmann, D., Chatonnet, A., Strähle, U., 2002. Acetylcholinesterase is required for neuronal and muscular development in the zebrafish embryo. *Nat. Neurosci.* 5, 111–118. <https://doi.org/10.1038/nn788>.
- Benfante, R., Di Lascio, S., Cardani, S., Fornasari, D., 2021. Acetylcholinesterase inhibitors targeting the cholinergic anti-inflammatory pathway: a new therapeutic perspective in aging-related disorders. *Aging Clin. Exp. Res.* 33, 823–834. <https://doi.org/10.1007/s40520-019-01359-4>.
- Berman, T., Hochner-Celnikier, D., Barr, D.B., Needham, L.L., Amitai, Y., Wormser, U., Richter, E., 2011. Pesticide exposure among pregnant women in Jerusalem, Israel: Results of a pilot study. *Environ. Int.* 37, 198–203. <https://doi.org/10.1016/j.envint.2010.09.002>.
- Bertero, A., Chiari, M., Vitale, N., Zanoni, M., Faggionato, E., Biancardi, A., Caloni, F., 2020. Types of pesticides involved in domestic and wild animal poisoning in Italy. *Sci. Total Environ.* 707, 136129. <https://doi.org/10.1016/j.scitotenv.2019.136129>.
- Bindea, G., Mlecnik, B., Hackl, H., Charoentong, P., Tosolini, M., Kirilovsky, A., Fridman, W.H., Pagès, F., Trajanoski, Z., Galon, J., 2009. ClueGO: A Cytoscape plugin to decipher functionally grouped gene ontology and pathway annotation networks. *Bioinformatics* 25, 1091–1093. <https://doi.org/10.1093/bioinformatics/btp101>.
- Blagden, C.S., Currie, P.D., Ingham, P.W., Hughes, S.M., 1997. Notochord induction of zebrafish slow muscle mediated by sonic hedgehog. *Genes Dev.* 11, 2163–2175. <https://doi.org/10.1101/gad.11.17.2163>.
- Bonsall, J.L., Goose, J., 1986. The safety evaluation of bendiocarb, a residual insecticide for vector control. *Toxicol. Lett.* 33, 45–59.
- Brannen, K.C., Panzica-Kelly, J.M., Danberry, T.L., Augustine-Rauch, K.A., 2010. Development of a zebrafish embryo teratogenicity assay and quantitative prediction model. *Birth Defects Res. Part B Dev. Reprod. Toxicol.* 89, 66–77. <https://doi.org/10.1002/bdrb.20223>.
- Brugueras, S., Fernández-Martínez, B., Martínez-de la Puente, J., Figuerola, J., Porro, T. M., Rius, C., Larrauri, A., Gómez-Barroso, D., 2020. Environmental drivers, climate change and emergent diseases transmitted by mosquitoes and their vectors in southern Europe: A systematic review. *Environ. Res.* 191, 110038. <https://doi.org/10.1016/j.envres.2020.110038>.
- Brunmeir, R., Lagger, S., Seiser, C., 2009. Histone deacetylase 1 and 2-controlled embryonic development and cell differentiation. *Int. J. Dev. Biol.* 53, 275–289. <https://doi.org/10.1387/ijdb.082649rb>.
- Bytyqi, A.H., Lockridge, O., Duysen, E., Wang, Y., Wolfrum, U., Layer, P.G., 2004. Impaired formation of the inner retina in an AChE knockout mouse results in degeneration of all photoreceptors. *Eur. J. of Neuroscience* 20, 2953–2962. <https://doi.org/10.1111/j.1460-9568.2004.03753.x>.
- Caminade, C., McIntyre, K.M., Jones, A.E., 2019. Impact of recent and future climate change on vector-borne diseases. *Ann. N. Y. Acad. Sci.* 1436, 157–173. <https://doi.org/10.1111/nyas.13950>.
- Cao, F., Souders, C.L., Li, P., Pang, S., Liang, X., Qiu, L., Martyniuk, C.J., 2019. Developmental neurotoxicity of maneb: notochord defects, mitochondrial dysfunction and hypoactivity in zebrafish (*Danio rerio*) embryos and larvae. *Ecotoxicol. Environ. Saf.* 170, 227–237. <https://doi.org/10.1016/j.ecoenv.2018.11.110>.
- Chang, C., Dai, Y., Zhang, J., Wu, Z., Li, S., Zhou, Z., 2024. Associations between exposure to pesticides mixture and semen quality among the non-occupationally exposed males: Four statistical models. *Environ. Res.* 257, 119400. <https://doi.org/10.1016/j.envres.2024.119400>.
- Chatonnet, A., Cousin, X., Stra, U., 2005. Are there non-catalytic functions of acetylcholinesterases? Lessons from mutant animal models. *Bioessays* 27, 189–200. <https://doi.org/10.1002/bies.20153>.
- Che, X., Huang, Y., Zhong, K., Jia, K., Wei, Y., Meng, Y., Yuan, W., Lu, H., 2023. Thiophanate-methyl induces notochord toxicity by activating the PI3K-mTOR pathway in zebrafish (*Danio rerio*) embryos. *Environ. Pollut.* 318, 120861. <https://doi.org/10.1016/j.envpol.2022.120861>.
- Cheng, B., Zhang, H., Hu, J., Peng, Y., Yang, J., Liao, X., Liu, F., Guo, J., Hu, C., Lu, H., 2020. The immunotoxicity and neurobehavioral toxicity of zebrafish induced by famoxadone-cymoxanil. *Chemosphere* 247, 125870. <https://doi.org/10.1016/j.chemosphere.2020.125870>.
- Cheng, B., Zou, L., Zhang, H., Cao, Z., Liao, X., Shen, T., Xiong, G., Xiao, J., Liu, H., Lu, H., 2021. Effects of cyhalofop-butyl on the developmental toxicity and immunotoxicity in zebrafish (*Danio rerio*). *Chemosphere* 263, 127849. <https://doi.org/10.1016/j.chemosphere.2020.127849>.
- Chopas-Konowalek, A., Zawadzki, M., Kurach, L., Wachelko, O., Ciaputa, R., Kaja, T., Pawel, S., 2022. Simultaneous use of 48 birds of prey-bendiocarb determination with the use of UHPLC-ESI-MS/MS method in fatal case from Eastern Europe. *Arch. Med. Sadowej Kryminol.* 72, 67–80. <https://doi.org/10.4467/16891716AMSJK.22.009.16807>.
- Correia, D., Almeida, A.R., Santos, J., Machado, A.L., Koba Ucin, O., Žlábek, V., Oliveira, M., Domingues, L., 2019. Behavioral effects in adult zebrafish after developmental exposure to carbaryl. *Chemosphere* 235, 1022–1029. <https://doi.org/10.1016/j.chemosphere.2019.07.029>.
- Dahanayake, P., Dassanayake, T.L., Pathirage, M., Gawarammana, I.B., Senanayake, S., Sedgwick, M., Weerasinghe, V.S., 2020. Dysfunction in macula, retinal pigment epithelium and post retinal pathway in acute organophosphorus poisoning. *Clin. Toxicol.* 59, 111–117. <https://doi.org/10.1080/15563650.2020.1771359>.
- Dinede, G., Bihon, W., Gazu, L., Foukmenio Mbokou, S., Girma, S., Srinivasan, R., Roothaert, R., Grace, D., Gashaw, H., Knight-Jones, T.J.D., 2023. Assessment of pesticide residues in vegetables produced in central and eastern Ethiopia. *Front. Sustain. Food Syst.* 7, 1143753. <https://doi.org/10.3389/fsufs.2023.1143753>.
- Ding, J., Dai, Y., Zhang, L., Wang, Z., Zhang, B., Guo, J., Qi, X., Lu, D., Chang, X., Wu, C., Zhang, J., Zhou, Z., 2024. Identifying childhood pesticide exposure trajectories and critical window associated with behavioral problems at 10 years of age: Findings from SMBCS. *Environ. Int.* 193, 109079. <https://doi.org/10.1016/j.envint.2024.109079>.
- Ellis, K., Bagwell, J., Bagnat, M., 2013. Notochord vacuoles are lysosome-related organelles that function in axis and spine morphogenesis. *J. Cell Biol.* 200, 667–679. <https://doi.org/10.1083/jcb.201212095>.
- Ellman, G.L., Courtney, K.D., Andres, V., Featherstone, R.M., 1961. A new and rapid colorimetric determination of acetylcholinesterase activity. *Biochem. Pharmacol.* 7, 88–95. [https://doi.org/10.1016/0006-2952\(61\)90145-9](https://doi.org/10.1016/0006-2952(61)90145-9).
- Fischer, A., Wolman, M., Granato, M., Parsons, M., McCallion, A.S., Proeschler, J., English, E., 2015. Carbamate nerve agent prophylactics exhibit distinct toxicological effects in the zebrafish embryo model. *Neurotoxicol. Teratol.* 50, 1–10. <https://doi.org/10.1016/j.ntt.2015.05.001>.
- Garry, V.F., Harkins, M.E., Erickson, L.L., Long-Simpson, L.K., Holland, S.E., Burroughs, B.L., 2002. Birth defects, season of conception, and sex of children born to pesticide applicators living in the Red River Valley of Minnesota, USA. *Environ. Health Perspect.* 110, 441–449. <https://doi.org/10.1289/ehp.02110s3441>.
- Gazsi, G., Czimmerer, Z., Ivánovics, B., Berta, I.R., Urbányi, B., Csenki-Bakos, Z., Ács, A., 2021. Physiological, developmental, and biomarker responses of zebrafish embryos to sub-lethal exposure of bendiocarb. *Water* 13, 204. <https://doi.org/10.3390/w13020204>.
- Gely-Permot, A., Saci, S., Kernanec, P.Y., Hao, C., Giton, F., Kervarrec, C., Tevosian, S., Mazaud-Guittot, S., Smagulova, F., 2017. Embryonic exposure to the widely-used herbicide atrazine disrupts meiosis and normal follicle formation in female mice. *Sci. Rep.* 7, 1–14. <https://doi.org/10.1038/s41598-017-03738-1>.
- Genge, C.E., Lin, E., Lee, L., Sheng, X.Y., Rayani, K., Gunawan, M., Stevens, C.M., Li, A.Y., Talab, S.S., Claydon, T.W., Hove-Madsen, L., Tibbits, G.F., 2016. The zebrafish heart

- as a model of mammalian cardiac function. *Rev. Physiol. Biochem. Pharmacol.* 171, 99–136. https://doi.org/10.1007/112_2016_5.
- Guilhermino, L., Lopes, M.C., Carvalho, A.P., Soares, A.M.V.M., 1996. Inhibition of acetylcholinesterase activity as effect criterion in acute tests with juvenile *Daphnia magna*. *Chemosphere* 32, 727–738. [https://doi.org/10.1016/0045-6535\(95\)00360-6](https://doi.org/10.1016/0045-6535(95)00360-6).
- Guo, R., Xing, Q.S., 2022. Roles of Wnt signaling pathway and ROR2 receptor in embryonic development: an update review article. *Epigenet. Insights* 15, 25168657211064230. <https://doi.org/10.1177/25168657211064232>.
- Haendel, M.A., Tilton, F., Bailey, G.S., Tanguay, R.L., 2004. Developmental toxicity of the dithiocarbamate pesticide sodium metam in Zebrafish. *Toxicol. Sci.* 81, 390–400. <https://doi.org/10.1093/toxsci/kfh202>.
- He, D., Han, G., Zhang, X., Sun, J., Xu, Y., Jin, Q., Gao, Q., 2022. Oxidative stress induced by methomyl exposure reduces the quality of early embryo development in mice. *Zygote* 30, 57–64. <https://doi.org/10.1017/S0967199421000277>.
- Hien, A.S., Soma, D.D., Sawadogo, S.P., Poda, S.B., Namountougou, M., Ouedraogo, G.A., Diabaté, A., Dabiré, R.K., 2020. Effect of bendiocarb (Ficam® 80% WP) on entomological indices of malaria transmission by indoor residual spraying in Burkina Faso, West Africa. *Adv. Entomol.* 8, 158–178. <https://doi.org/10.4236/ae.2020.84012>.
- Hill, A.J., Teraoka, H., Heideman, W., Peterson, R.E., 2005. Zebrafish as a model vertebrate for investigating chemical toxicity. *Toxicol. Sci.* 86, 6–19. <https://doi.org/10.1093/toxsci/kfi110>.
- Holovska, K., Almasiova, V., Cigankova, V., 2014. Ultrastructural changes in the rabbit liver induced by carbamate insecticide bendiocarb. *J. Environ. Sci. Heal. Part B* 49, 616–623. <https://doi.org/10.1080/03601234.2014.911593>.
- Holovská, K., Almäšiová, V., Tarabová, L., Petrovová, E., Cigánková, V., 2017. Effect of the bendiocarb on the ultrastructure of rabbit skeletal muscle. *Acta Vet. Brno* 86, 219–222. <https://doi.org/10.2754/avb201786030219>.
- Horzmann, K.A., Freeman, J.L., 2018. Making waves: New developments in toxicology with the zebrafish. *Toxicol. Sci.* 163, 5–12. <https://doi.org/10.1093/toxsci/kfy044/4870163>.
- Howe, K., Clark, M.D., Torroja, C.F., Torrance, J., Berthelot, C., Muffato, M., Collins, J.E., Humphray, S., McLaren, K., Matthews, L., McLaren, S., Sealy, I., Caccamo, M., Churcher, C., Scott, C., Barrett, J.C., Koch, R., Rauch, G.-J., White, S., Chow, W., Kilian, B., Quintais, L.T., Guerra-Assunção, J.A., Zhou, Y., Gu, Y., Yen, J., Vogel, J.-H., Eyre, T., Redmond, S., Banerjee, R., Chi, J., Fu, B., Langley, E., Magueire, S.F., Laird, G.K., Lloyd, D., Kenyon, E., Donaldson, S., Sehra, H., Almeida-King, J., Loveland, J., Trevanion, S., Jones, M., Quail, M., Willey, D., Hunt, A., Burton, J., Sims, S., McLay, K., Plumb, B., Davis, J., Clee, C., Oliver, K., Clark, R., Riddle, C., Elliott, D., Threadgold, G., Harden, G., Ware, D., Begum, S., Mortimore, B., Kerry, G., Heath, P., Phillimore, B., Tracey, A., Corby, N., Dunn, M., Johnson, C., Wood, J., Clark, S., Pelan, S., Griffiths, G., Smith, M., Glithero, R., Howden, P., Barker, N., Lloyd, C., Stevens, C., Harley, J., Holt, K., Panagiotidis, G., Lovell, J., Beasley, H., Henderson, C., Gordon, D., Auger, K., Wright, D., Collins, J., Raisen, C., Dyer, L., Leung, K., Robertson, L., Ambridge, K., Leongamornlert, D., McGuire, S., Gildetherp, R., Griffiths, C., Manthorpe, D., Nichol, S., Barker, G., Whitehead, S., Kay, M., Brown, J., Murnane, C., Gray, E., Humphries, M., Sycamore, N., Barker, D., Saunders, D., Wallis, J., Babbage, A., Hammond, S., Mashreghi-Mohammadi, M., Barr, L., Martin, S., Wray, P., Ellington, A., Matthews, N., Ellwood, M., Woodmansey, R., Clark, G., Cooper, J.D., Tromans, A., Grafham, D., Skuce, C., Pandian, R., Andrews, R., Harrison, E., Kimberley, A., Garnett, J., Fosker, N., Hall, R., Garner, P., Kelly, D., Bird, C., Palmer, S., Gehring, I., Berger, A., Dooley, C. M., Ersan-Urün, Z., Eser, C., Geiger, H., Geisler, M., Karotki, L., Kirn, A., Konantz, J., Konantz, M., Oberländer, M., Rudolph-Geiger, S., Teucke, M., Lanz, C., Raddatz, G., Osoegawa, K., Zhu, B., Rapp, A., Widawa, S., Langford, C., Yang, F., Schuster, S.C., Carter, N.P., Harrow, J., Ning, Z., Herrero, J., Searle, S.M.J., Enright, A., Geisler, R., Plasterk, R.H.A., Lee, C., Westerfield, M., de Jong, P.J., Zon, L.I., Postlethwait, J.H., Nüsslein-Volhard, C., Hubbard, T.J.P., Roest Crolius, H., Rogers, J., Stemple, D.L., 2013. The zebrafish reference genome sequence and its relationship to the human genome. *Nature* 496, 498–503. <https://doi.org/10.1038/nature12111>.
- Howell, G.E., Kondakala, S., Holdridge, J., Lee, J.H., Ross, M.K., 2018. Inhibition of cholinergic and non-cholinergic targets following subacute exposure to chlorpyrifos in normal and high fat fed male C57BL/6J mice. *Food Chem. Toxicol.* 118, 821–829. <https://doi.org/10.1016/j.fct.2018.06.051>.
- Illsinger, S., Das, A.M., 2010. Impact of selected inborn errors of metabolism on prenatal and neonatal development. *IUBMB Life* 62, 403–413. <https://doi.org/10.1002/iub.336>.
- Ishido, M., Suzuki, J., Masuo, Y., 2017. Neonatal rotenone lesions cause onset of hyperactivity during juvenile and adulthood in the rat. *Toxicol. Lett.* 266, 42–48. <https://doi.org/10.1016/j.toxlet.2016.12.008>.
- Ivanovics, B., Gazsi, G., Reining, M., Berta, I., Poliska, S., Toth, M., Domokos, A., Nagy, B., Staszny, A., Cserhati, M., Csosz, E., Bacs, A., Csenki-Bakos, Z., Acs, A., Urbanyi, B., Czimmerer, Z., 2021. Embryonic exposure to low concentrations of aflatoxin B1 triggers global transcriptomic changes, defective yolk lipid mobilization, abnormal gastrointestinal tract development and inflammation in zebrafish. *J. Hazard. Mater.* 416, 125788. <https://doi.org/10.1016/j.jhazmat.2021.125788>.
- Jablonski, C.A., Pereira, T.C.B., Teodoro, L.D.S., Altenhofen, S., Rübensam, G., Bonan, C. D., Bogo, M.R., 2022. Acute toxicity of methomyl commercial formulation induces morphological and behavioral changes in larval zebrafish (*Danio rerio*). *Neurotoxicol. Teratol.* 89, 107058. <https://doi.org/10.1016/j.ntt.2021.107058>.
- Jiang, Y., Swale, D., Carlier, P.R., Hartsel, J.A., Ma, M., Ekström, F., Bloomquist, J.R., 2013. Evaluation of novel carbamate insecticides for neurotoxicity to non-target species. *Pestic. Biochem. Physiol.* 106, 156–161. <https://doi.org/10.1016/j.pestbp.2013.03.006>.
- Kamboj, A., Sandhir, R., 2007. Perturbed synaptosomal calcium homeostasis and behavioral deficits following carbofuran exposure: Neuroprotection by N-acetylcysteine. *Neurochem. Res.* 32, 507–516. <https://doi.org/10.1007/s11064-006-9264-y>.
- Kamboj, A., Kiran, R., Sandhir, R., 2006. Carbofuran-induced neurochemical and neurobehavioral alterations in rats: Attenuation by N-acetylcysteine. *Exp. Brain Res.* 170, 567–575. <https://doi.org/10.1007/s00221-005-0241-5>.
- Klingenberg, C.P., 2011. MorphoJ: An integrated software package for geometric morphometrics. *Mol. Ecol. Resour.* 11, 353–357. <https://doi.org/10.1111/j.1755-0998.2010.02924.x>.
- Klüver, N., Yang, L., Busch, W., Scheffler, K., Renner, P., Strähle, U., Scholz, S., 2011. Transcriptional response of zebrafish embryos exposed to neurotoxic compounds reveals a muscle activity dependent hspb11 expression. *PLoS One* 6, e29063. <https://doi.org/10.1371/journal.pone.0029063>.
- Krockova, J., Massányi, P., Toman, R., Danko, J., Roychoudhury, S., 2012. In vivo and in vitro effect of bendiocarb on rabbit testicular structure and spermatozoa motility. *J. Environ. Sci. Health A* 47, 1301–1311. <https://doi.org/10.1080/10934529.2012.672136>.
- Külp, F.O., Doğançift, İ., 2021. Effects of Bendiocarb Insecticide on Lipid Peroxidation, Antioxidant Enzymes and DNA Damage in Human Leucocytes. *Erciyes Üniversitesi Fen Bilim. Enstitüsü Fen Bilim. Derg.* 37, 348–355.
- Kuraguchi, M., Wang, X., Bronson, R.T., Rothenberg, R., Ohene-baah, N.Y., Lund, J.J., Kucherlapati, M., Maas, R.L., Kucherlapati, R., 2006. Adenomatous polyposis coli (APC) is required for normal development of skin and thymus. *PLoS Genet.* 2, e146. <https://doi.org/10.1371/journal.pgen.0020146>.
- Lee, I., Eriksson, P., Fredriksson, A., Buratovic, S., Viberg, H., 2015. Developmental neurotoxic effects of two pesticides: Behavior and biomolecular studies on chlorpyrifos and carbaryl. *Toxicol. Appl. Pharmacol.* 288, 429–438. <https://doi.org/10.1016/j.taap.2015.08.014>.
- Lee, S., Barron, M.G., 2016. A mechanism-based 3D-QSAR approach for classification and prediction of acetylcholinesterase inhibitory potency of organophosphate and carbamate analogs. *J. Comput. Aided Mol. Des.* 30, 347–363. <https://doi.org/10.1007/s10822-016-9910-7>.
- Lefebvre, J.L., Ono, F., Puglielli, C., Seidner, G., Franzini-Armstrong, C., Brehm, P., Granato, M., 2004. Increased neuromuscular activity causes axonal defects and muscular degeneration. *Development* 131, 2605–2618. <https://doi.org/10.1242/dev.01123>.
- Lepiller, S., Laurens, V., Bouchot, A., Herbomel, P., Solary, E., Chlubá, J., 2007. Imaging of nitric oxide in a living vertebrate using a diaminofluorescein probe. *Free Radic. Biol. Med.* 43, 619–627. <https://doi.org/10.1016/j.freeradbiomed.2007.05.025>.
- Levin, B.E., 2006. Metabolic imprinting: critical impact of the perinatal environment on the regulation of energy homeostasis. *Philos. Trans. R. Soc. B* 361, 1107–1121. <https://doi.org/10.1098/rstb.2006.1851>.
- Li, W., Cornell, R.A., 2007. Redundant activities of Tfp2a and Tfp2c are required for neural crest induction and development of other non-neural ectoderm derivatives in zebrafish embryos. *Dev. Biol.* 304, 338–354. <https://doi.org/10.1016/j.ydbio.2006.12.042>.
- Liao, C. yuan, Yi, X. lei, Yang, Y. xin, Gong, J. min, Ma, Y.L., Long, F., Liu, Z. zhong, Du, Z., 2025. Evaluation of the inhibitory effects of carbamate pesticides on human carboxylesterases. *Toxicol. Appl. Pharmacol.* 502, 117454. <https://doi.org/10.1016/j.taap.2025.117454>.
- Liu, Q., Zhang, X., Qin, Y., Yi, J., Li, J., 2020b. Acetylcholinesterase inhibition ameliorates retinal neovascularization and glial activation in oxygen-induced retinopathy. *Int. J. Ophthalmol.* 13, 1361. <https://doi.org/10.18240/ijo.2020.09.04>.
- Liu, S., Yu, M., Xie, X., Ru, Y., Ru, S., 2020a. Carbofuran induces increased anxiety-like behaviors in female zebrafish (*Danio rerio*) through disturbing dopaminergic/norepinephrine system. *Chemosphere* 253, 126635. <https://doi.org/10.1016/j.chemosphere.2020.126635>.
- Lo, C., Dia, A.K., Dia, I., Niang, E.H.A., Konaté, L., Faye, O., 2019. Evaluation of the residual efficacy of indoor residual spraying with bendiocarb (FICAM WP 80) in six health districts in Senegal. *Malar. J.* 18, 1–10. <https://doi.org/10.1186/s12936-019-2829-4>.
- Manikkam, M., Haque, M.M., Guerrero-Bosagna, C., Nilsson, E.E., Skinner, M.K., 2014. Pesticide methoxychlor promotes the epigenetic transgenerational inheritance of adult-onset disease through the female germline. *PLoS One* 9, e102091. <https://doi.org/10.1371/journal.pone.0102091>.
- Mathias, J.R., Perrin, B.J., Liu, T.-X., Kanki, J., Look, A.T., Huttenlocher, A., 2006. Resolution of inflammation by retrograde chemotaxis of neutrophils in transgenic zebrafish. *J. Leukoc. Biol.* 80, 1281–1288. <https://doi.org/10.1189/jlb.0506346>.
- Matthews, M., Varga, Z.M., 2012. Anesthesia and euthanasia in zebrafish. *ILAR J.* 53, 192–204. <https://doi.org/10.1093/ilar.53.2.192>.
- Meng, S.L., Li, M.X., Lu, Y., Chen, X., Wang, W.P., Song, C., Fan, L.M., Qiu, L.P., Li, D.D., Xu, H.M., Xu, P., 2023. Effect of environmental level of methomyl on hatching, morphology, immunity and development related genes expression in zebrafish (*Danio rerio*) embryo. *Ecotoxicol. Environ. Saf.* 268, 115684. <https://doi.org/10.1016/j.ecoenv.2023.115684>.
- Mishra, Tiwari, S.K., Agarwal, S., Sharma, V.P., Chaturvedi, R.K., 2012. Prenatal carbofuran exposure inhibits hippocampal neurogenesis and causes learning and memory deficits in offspring. *Toxicol. Sci.* 127, 84–100. <https://doi.org/10.1093/toxsci/kfs004>.
- Montgomery, M.P., Postel, E., Umbach, D.M., Richards, M., Watson, M., Blair, A., Chen, H., Sandler, D.P., Schmidt, S., Kamel, F., 2005. Pesticide use and age-related macular degeneration in the agricultural health study. *Environ. Health Perspect.* 113, 077013.
- Nasiadka, A., Clark, M.D., 2012. Zebrafish breeding in the laboratory environment. *ILAR J.* 53, 161–168. <https://doi.org/10.1093/ilar.53.2.161>.

- Nayak, P.K., Subramanian, A., Schilling, T.F., 2025. Transcriptome profiling of tendon fibroblasts at the onset of embryonic muscle contraction reveals novel force-responsive genes. *Elife* 14, e105802.
- Nishimura, Y., Inoue, A., Sasagawa, S., Koikiwa, J., Kawaguchi, K., Kawase, R., Maruyama, T., Kim, S., Tanaka, T., 2016. Using zebrafish in systems toxicology for developmental toxicity testing. *Congenit. Anom.* 56, 18–27. <https://doi.org/10.1111/cga.12142>. Kyoto.
- Ochi, H., Westerfield, M., 2007. Signaling networks that regulate muscle development: Lessons from zebrafish. *Develop. Growth Differ.* 49, 1–11. <https://doi.org/10.1111/j.1440-169X.2007.00905.x>.
- OECD, 2025. Test No. 236: Fish Embryo Acute Toxicity (FET) Test, OECD Guidelines for the Testing of Chemicals, Section 2. OECD Publishing, Paris. <https://doi.org/10.1787/9789264203709-en>.
- Oehlers, S.H., Flores, M.V., Hall, C.J., Okuda, K.S., Sison, J.O., Crosier, K.E., Crosier, P.S., 2013. Chemically induced intestinal damage models in zebrafish larvae. *Zebrafish* 10, 184–193. <https://doi.org/10.1089/zeb.2012.0824>.
- Ornoy, A., 2006. Neuroteratogens in man: An overview with special emphasis on the teratogenicity of antiepileptic drugs in pregnancy. *Reprod. Toxicol.* 22, 214–226. <https://doi.org/10.1016/j.reprotox.2006.03.014>.
- Ostrea, E.M., Reyes, A., Villanueva-Uy, E., Pacifico, R., Benitez, B., Ramos, E., Bernardo, R.C., Bielawski, D.M., Delaney-Black, V., Chiodo, L., Janisse, J.J., Ager, J. W., 2012. Fetal exposure to propoxur and abnormal child neurodevelopment at 2 years of age. *Neurotoxicology* 33, 669–675. <https://doi.org/10.1016/j.neuro.2011.11.006>.
- Pelkonen, O., Vähäkangas, K., Gupta, R.C., 2006. Placental Toxicity of Organophosphate and Carbamate Pesticides. *Toxicology of Organophosphate & Carbamate Compounds*. 463–479. <https://doi.org/10.1016/B978-012088523-7/50034-X>.
- Pelletier, M., Roberge, C.J., Gauthier, M., Vandal, K., Tessier, P.A., Girard, D., 2001. Activation of human neutrophils in vitro and dieldrin-induced neutrophilic inflammation in vivo. *J. Leukoc. Biol.* 70, 367–373. <https://doi.org/10.1189/jlb.70.3.367>.
- Penton, A.L., Leonard, L.D., Spinner, N.B., 2012. Notch signaling in human development and disease. *Semin. Cell Dev. Biol.* 23, 450–457. <https://doi.org/10.1016/j.semcdb.2012.01.010>.
- Petrovova, E., Sedmera, D., Lesnik, F., Luptakova, L., 2009. Bendiocarb effect on liver and central nervous system in the chick embryo. *J. Environ. Sci. Heal. Part B* 44, 383–388. <https://doi.org/10.1080/03601230902801091>.
- Petrovova, E., Mazensky, D., Luptakova, L., Holovska, K., Spalekova, E., Massanyi, P., Haladova, E., Toth, T., 2010a. Alterations in the rabbit lymphoid tissue after bendiocarb administration. *J. Environ. Sci. Health B* 45, 718–727. <https://doi.org/10.1080/03601234.2010.502465>.
- Petrovova, E., Maženský, D., Vdoviaková, K., Massanyi, P., Luptáková, L., Smrčo, P., 2010b. Effect of bendiocarb on development of the chick embryo. *J. Appl. Toxicol.* 30, 397–401. <https://doi.org/10.1002/jat.1509>.
- Petrovova, E., Massanyi, P., Capcarova, M., Zivcak, J., Stodola, L., 2011. Structural alterations in rabbit spleen after bendiocarb administration. *J. Environ. Sci. Heal. Part B* 46, 788–792. <https://doi.org/10.1080/03601234.2012.601937>.
- Petrovova, E., Sedmera, D., Luptakova, L., Mazensky, D., Danko, J., 2012. Chick development and high dose of bendiocarb. *J. Environ. Sci. Heal. Part A* 47, 1312–1318. <https://doi.org/10.1080/10934529.2012.672138>.
- Prahl, M., Odorizzi, P., Gingrich, D., Muhindo, M., McIntyre, T., Budker, R., Jagannathan, P., Farrington, L., Nalubega, M., Nankya, F., Sikyomu, E., Musinguzi, K., Naluwu, K., Auma, A., Kakuru, A., Kanya, M.R., Dorsey, G., Aweka, F., Feeney, M.E., 2021. Exposure to pesticides in utero impacts the fetal immune system and response to vaccination in infancy. *Nat. Commun.* 12, 132. <https://doi.org/10.1038/s41467-020-20475-8>.
- Pu, J., Wang, Z., Chung, H., 2020. Climate change and the genetics of insecticide resistance. *Pest Manag. Sci.* 76, 846–852. <https://doi.org/10.1002/ps.5700>.
- Rohlf, F.J., 2010a. tpsUtil, file utility program, version 1.46.
- Rohlf, F.J., 2010b. tps-DIG, digitize landmarks and outlines, version 2.16.
- Saeid, M.H.E., Turki, A.M.A., Wable, M.I.A., Nasser, G.A., 2011. Evaluation of pesticide residues in Saudi Arabia ground water. *Res. J. Environ. Sci.* 5, 171–178. <https://doi.org/10.3923/rjes.2011.171.178>.
- Sell, B., Sniegocki, T., Giergiel, M., Andrzej, P., 2022. White-tailed eagles (*Haliaeetus albicilla*) exposure to anticoagulant rodenticides and causes of poisoning in Poland (2018–2020). *Toxics* 10, 63.
- Seomoon, K., Park, J., Song, G., Lim, W., 2025. Environmental and toxicological effects of carbamate pesticides on zebrafish embryogenesis. *Mol. Cell. Toxicol.* 1–11. <https://doi.org/10.1007/s13273-025-00534-1>.
- Seth, B., Yadav, A., Tandon, A., Shankar, J., Chaturvedi, R.K., 2019. Carbofuran hampers oligodendrocytes development leading to impaired myelination in the hippocampus of rat brain. *Neurotoxicology* 70, 161–179. <https://doi.org/10.1016/j.neuro.2018.11.007>.
- Shukla, A., Malhotra, S., Kumar, M., Singla, N., 2022. Pesticides and human health: The noxious impact on maternal system and fetal development. *Pesticides in the Natural Environment*. 209–226.
- Shwartz, Y., Farkas, Z., Stern, T., Aszodi, A., Zelzer, E., 2012. Muscle contraction controls skeletal morphogenesis through regulation of chondrocyte convergent extension. *Dev. Biol.* 370, 154–163. <https://doi.org/10.1016/j.ydbio.2012.07.026>.
- Stehr, C.M., Linbo, T.L., Incardona, J.P., Scholz, N.L., 2006. The developmental neurotoxicity of fipronil: Notochord degeneration and locomotor defects in zebrafish embryos and larvae. *Toxicol. Sci.* 92, 270–278. <https://doi.org/10.1093/toxsci/kfj185>.
- Stevanović, N., Idbea, W., Bošković, J., Prodanović, R., Vapa, I., 2024. Pesticide residues in different honey types and public health risk assessment. *Acta Vet. Brno* 93, 105–114.
- Strähle, U., Scholz, S., Geisler, R., Greiner, P., Hollert, H., Rastegar, S., Schumacher, A., Selderslaghs, I., Weiss, C., Witters, H., Braunbeck, T., 2012. Zebrafish embryos as an alternative to animal experiments—A commentary on the definition of the onset of protected life stages in animal welfare regulations. *Reprod. Toxicol.* 33, 128–132. <https://doi.org/10.1016/j.reprotox.2011.06.121>.
- Suarez-Lopez, J.R., Himes, J.H., Jacobs, D.R., Alexander, B.H., Gunnar, M.R., 2013. Acetylcholinesterase activity and neurodevelopment in boys and girls. *Pediatrics* 132, 1649–1658. <https://doi.org/10.1542/peds.2013-0108>.
- Thawer, N.G., Ngondi, J.M., Mugalura, F.E., Emmanuel, I., Mwalimu, C.D., Morou, E., Vontas, J., Protopopoff, N., Rowland, M., Mutagahywa, J., Lalji, S., Molteni, F., Ramsan, M.M., Willilo, R., Wright, A., Kafuko, J.M., Ndong, I., Reithinger, R., Magesa, S.M., 2015. Use of insecticide quantification kits to investigate the quality of spraying and decay rate of bendiocarb on different wall surfaces in Kagera region, Tanzania. *Parasit. Vectors* 8, 1–10. <https://doi.org/10.1186/s13071-015-0859-5>.
- Tsiaoussis, J., Hatzidaki, E., Docea, A.O., Nikolouzakis, T.K., Petrakis, D., Burykina, T., Mamoulakis, C., Makrigiannakis, A., Tsatsakis, A., 2018. Molecular and clinical aspects of embryotoxicity induced by acetylcholinesterase inhibitors. *Toxicology* 409, 137–143. <https://doi.org/10.1016/j.tox.2018.07.018>.
- van den Berg, H., da Silva Bezerra, H.S., Al-Eryani, S., Chanda, E., Nagpal, B.N., Knox, T. B., Velayudhan, R., Yadav, R.S., 2021. Recent trends in global insecticide use for disease vector control and potential implications for resistance management. *Sci. Rep.* 11, 23867. <https://doi.org/10.1038/s41598-021-03367-9>.
- WM-Bekele, D., GirmaTilahun, Dadebo, E., Haileslassie, A., Gebremariam, Z., 2024. Organochlorine, organophosphorus, and carbamate pesticide residues in an Ethiopian Rift Valley Lake Hawassa: occurrences and possible ecological risks. *Environ. Sci. Pollut. Res.* 31, 27749–27769. <https://doi.org/10.1007/s11356-024-32848-3>.
- Xie, Y., Meijer, A.H., Schaaf, M.J.M., 2021. Modeling inflammation in Zebrafish for the development of anti-inflammatory drugs. *Front. Cell Dev. Biol.* 8, 1819. <https://doi.org/10.3389/fcell.2020.620984>.
- Xu, H., Zhang, X., Li, H., Li, C., Huo, X.J., Hou, L.P., Gong, Z., 2018. Immune response induced by major environmental pollutants through altering neutrophils in zebrafish larvae. *Aquat. Toxicol.* 201, 99–108. <https://doi.org/10.1016/j.aquatox.2018.06.002>.
- Zhang, J., Guo, J., Wu, C., Qi, X., Jiang, S., Lv, S., Lu, D., Liang, W., Chang, X., Zhang, Y., Cao, Y., Zhou, Z., 2022. Carbamate pesticides exposure and delayed physical development at the age of seven: Evidence from the SMBCS study. *Environ. Int.* 160, 107076. <https://doi.org/10.1016/j.envint.2022.107076>.
- Zhang, Y., Jin, C., Wang, X., Shen, M., Zhou, J., Wu, S., Fu, Z., Jin, Y., 2018. Propamocarb exposure decreases the secretion of neurotransmitters and causes behavioral impairments in mice. *Environ. Toxicol.* 34, 22–29. <https://doi.org/10.1002/tox.22653>.
- Zhou, C., Wang, X., Han, Z., Wang, D., Ma, Y., Liang, C.-G., 2019. Loss of CENPF leads to developmental failure in mouse embryos. *Cell Cycle* 18, 2784–2799. <https://doi.org/10.1080/15384101.2019.1661173>.